Neural Dense Non-Rigid Structure from Motion with Latent Space Constraints

Vikramjit Sidhu [1, 2] Edgar Tretschk [1]
Vladislav Golyanik [1] Antonio Agudo [3] Christian Theobalt [1]

[1] Max Planck Institute for Informatics, SIC [2] Saarland University, SIC
[3] Institut de Robòtica i Informàtica Industrial, CSIC-UPC

Non-Rigid Structure from Motion

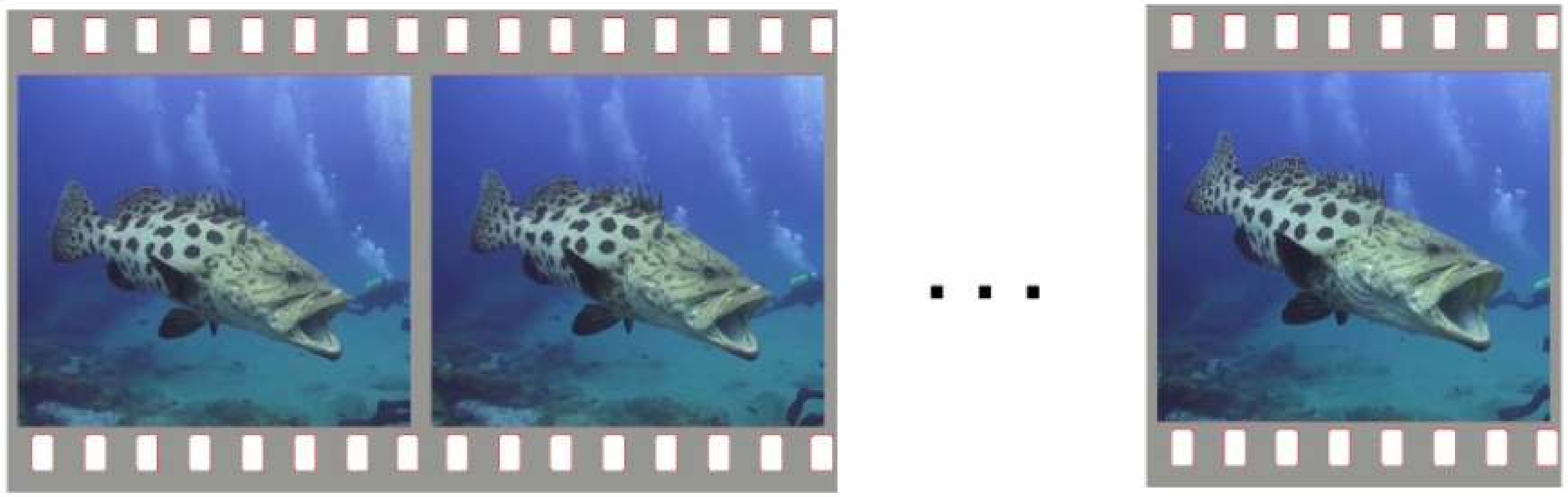

input monocular video

Non-Rigid Structure from Motion

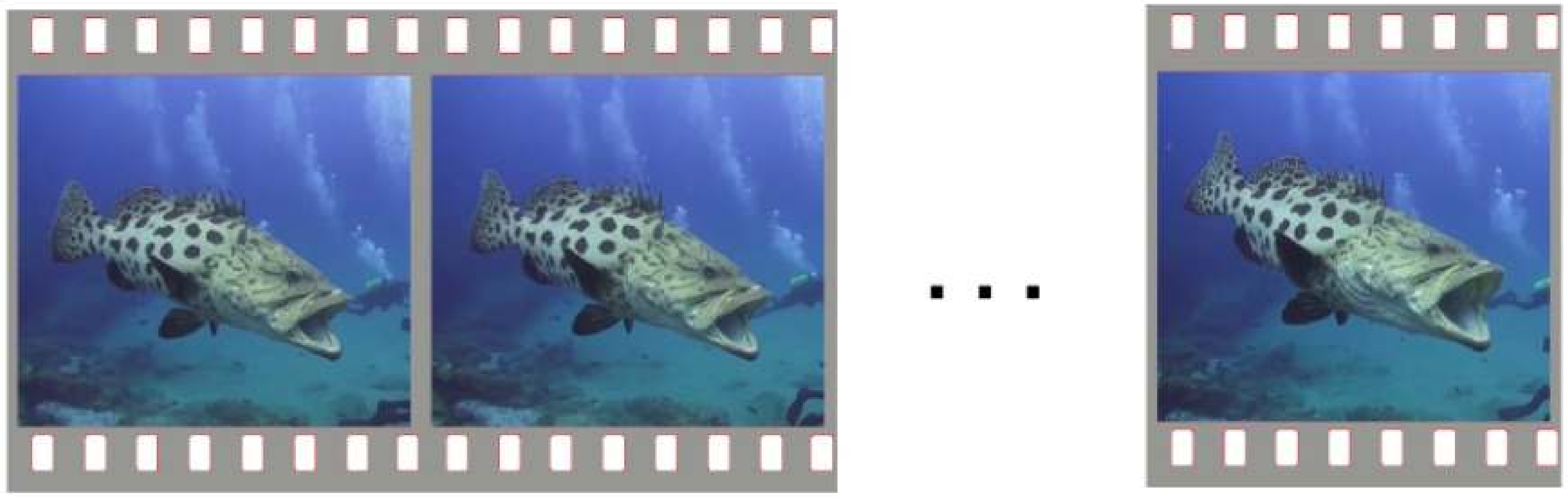

input monocular video

corresponding 3D reconstructions

Non-Rigid Structure from Motion

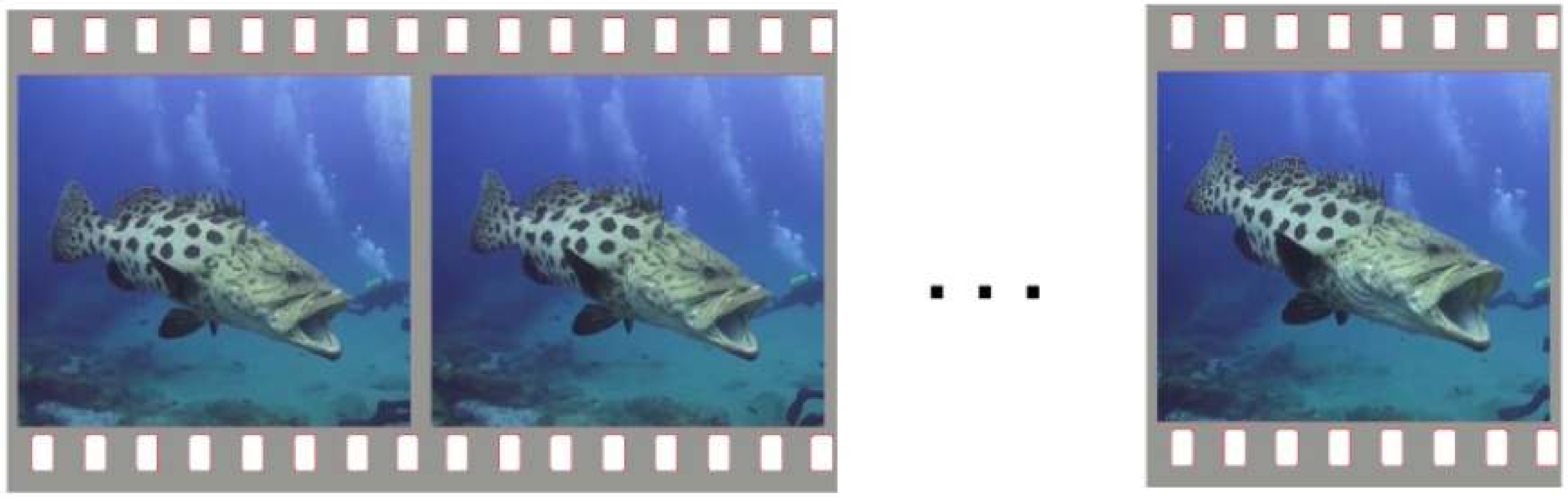

input monocular video

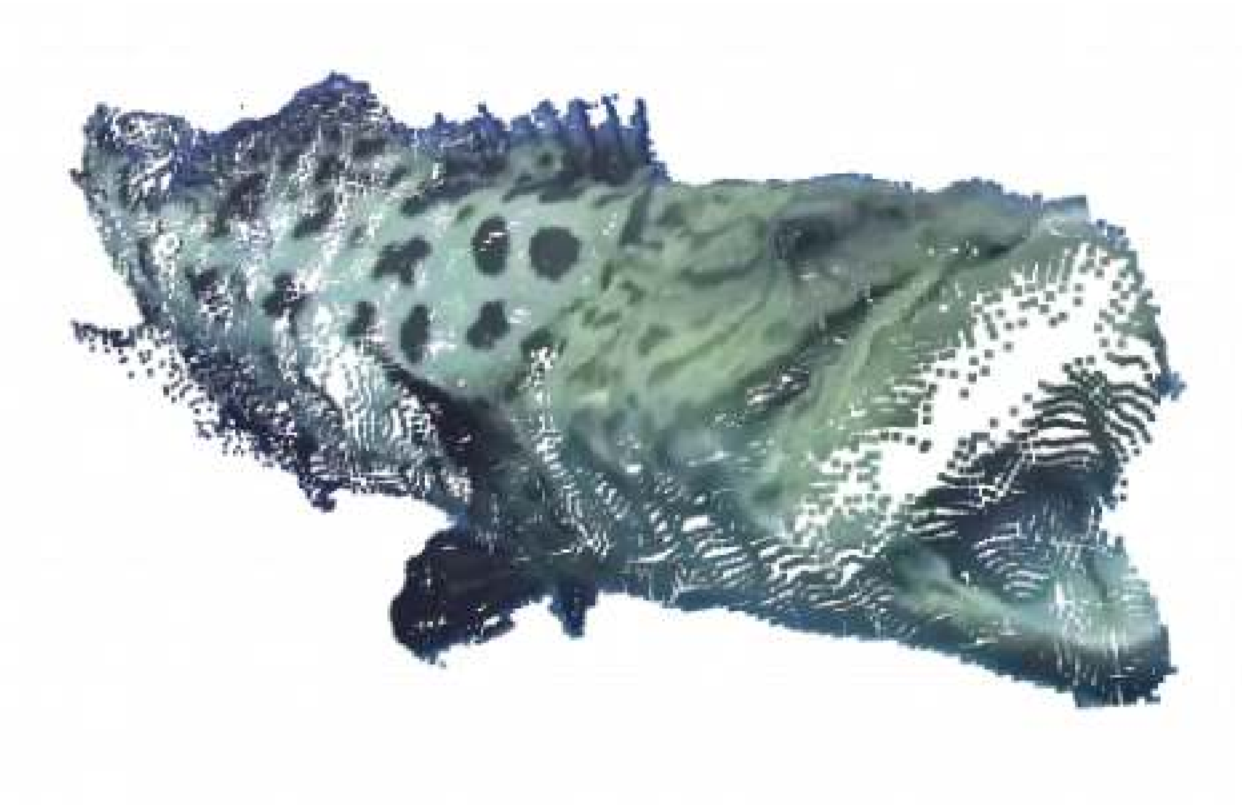

corresponding 3D reconstructions

Non-Rigid Structure from Motion

Non-Rigid Structure from Motion

Non-Rigid Structure from Motion

Non-Rigid Structure from Motion

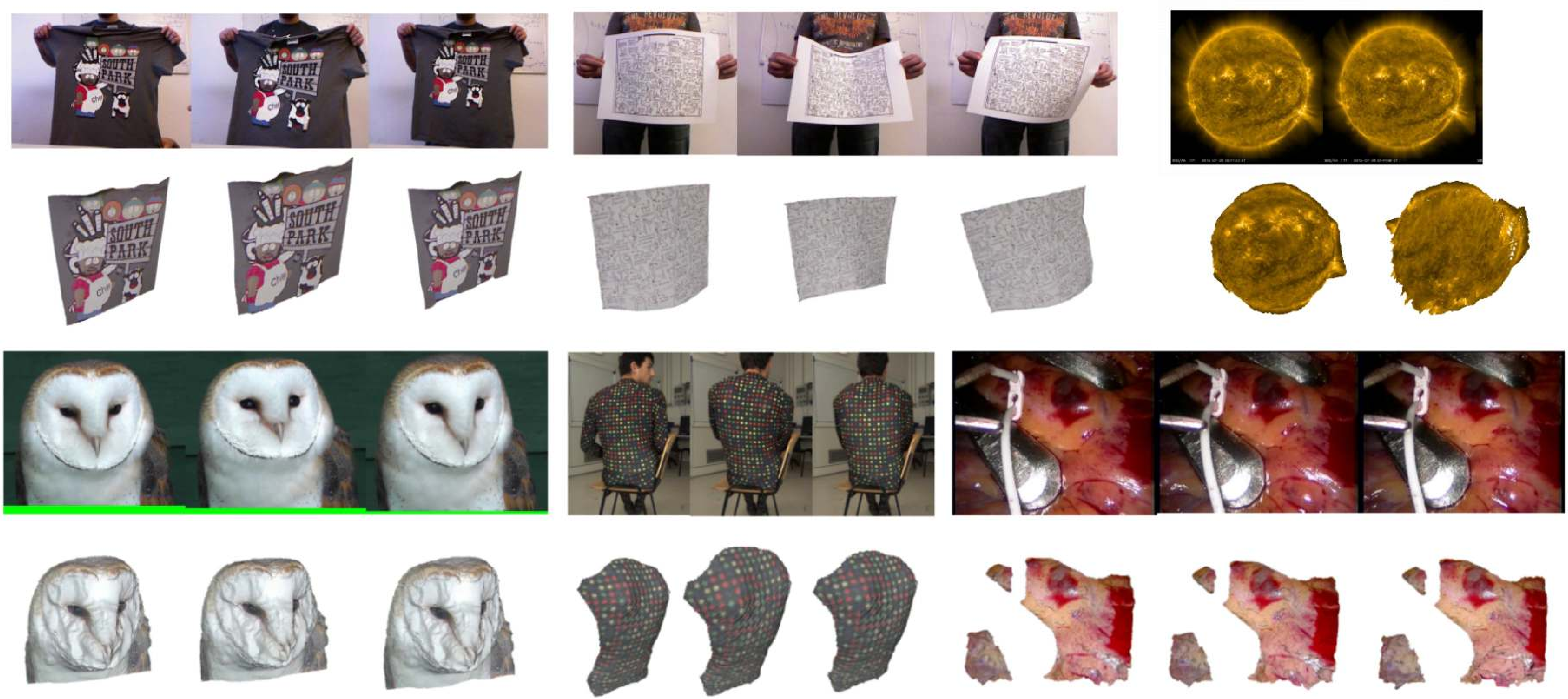

Non-Rigid Structure from Motion

input frame

Non-Rigid Structure from Motion

input frame

3D reconstructions by different NRSfM methods

Which 3D Reconstruction is Accurate?

input frame

3D reconstructions by different NRSfM methods

Non-Rigid Structure from Motion

line

flyby

zigzag

Dataset: S.H.N. Jensen *et al.* arXiv.org, 2018.
Applied Method: V. Golyanik *et al.*, arXiv.org, 2019.

Non-Rigid Structure from Motion

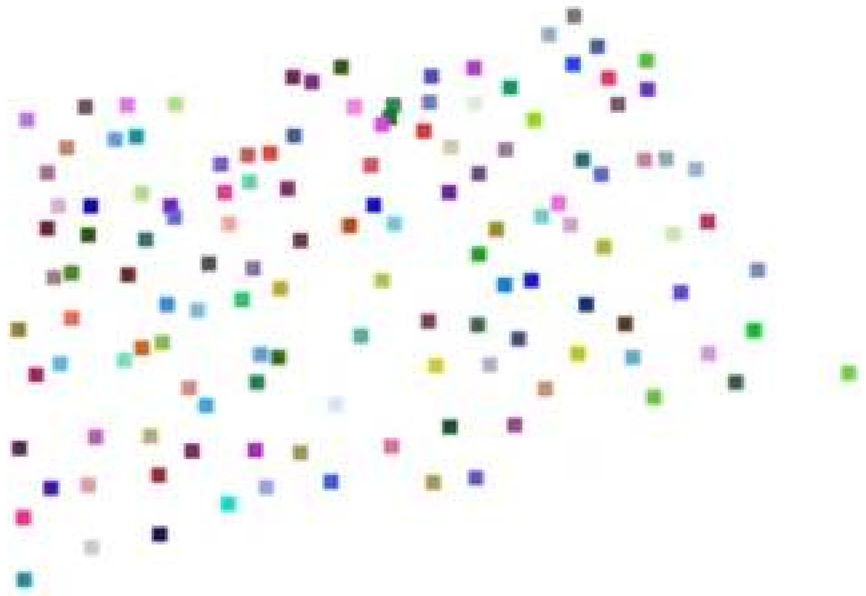

semi-circle

zigzag

tricky

Dataset: S.H.N. Jensen *et al.* arXiv.org, 2018.
Applied Method: V. Golyanik *et al.*, arXiv.org, 2019.

Non-Rigid Structure from Motion

Dataset: S.H.N. Jensen *et al.* arXiv.org, 2018.
Applied Method: V. Golyanik *et al.*, arXiv.org, 2019.

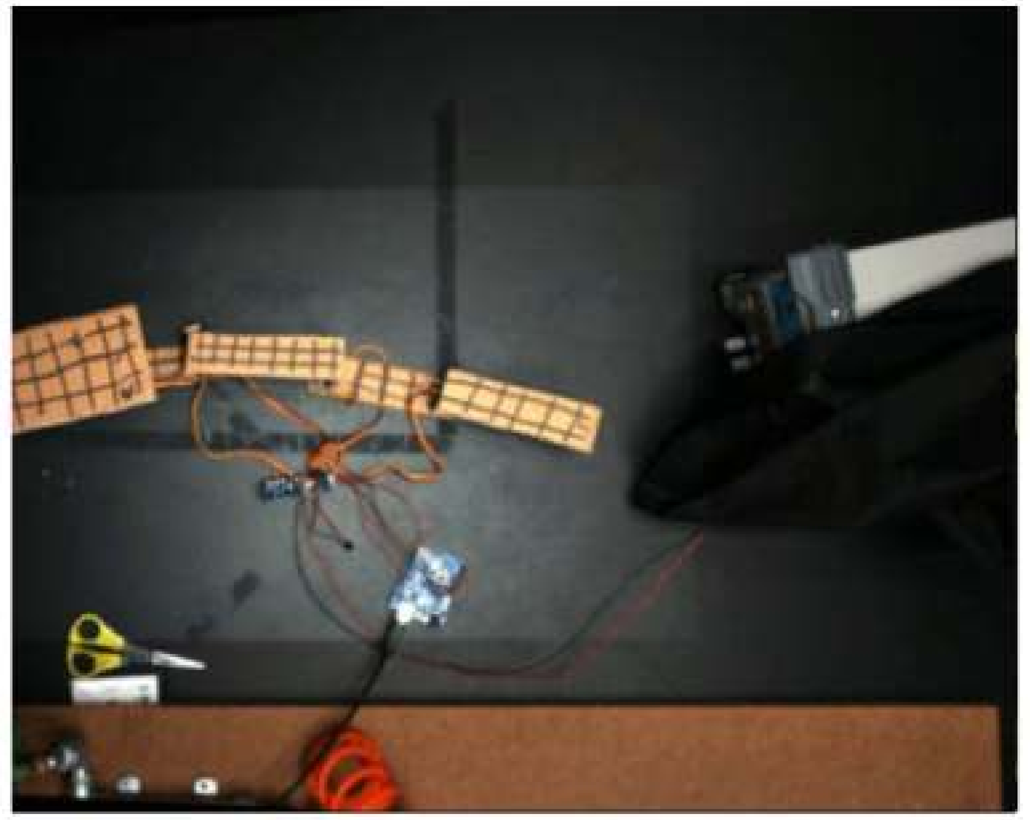

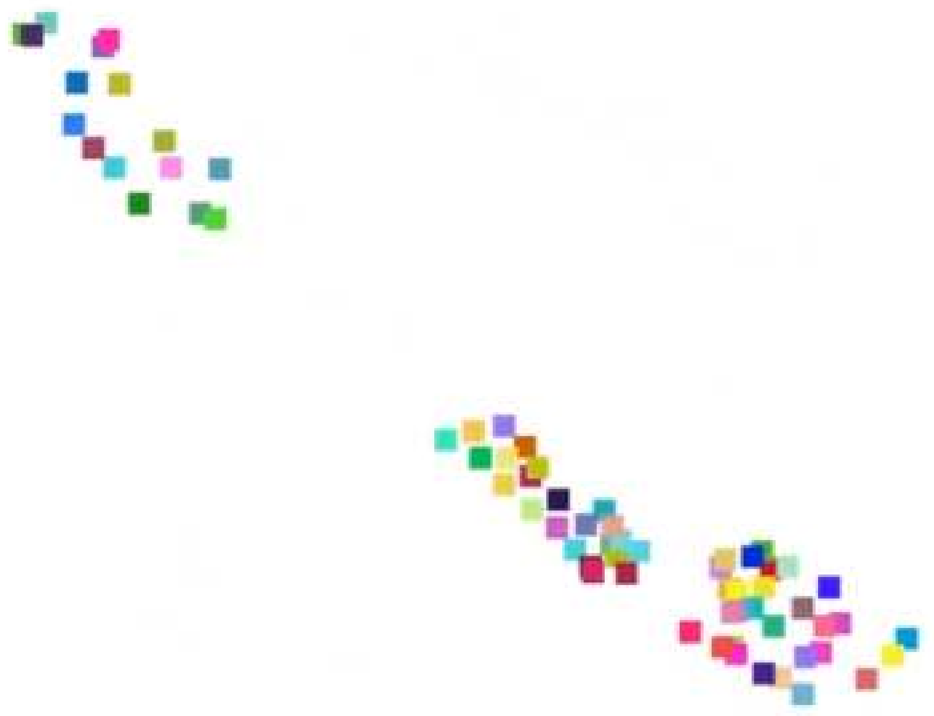

circle

flyby

Non-Rigid Structure from Motion

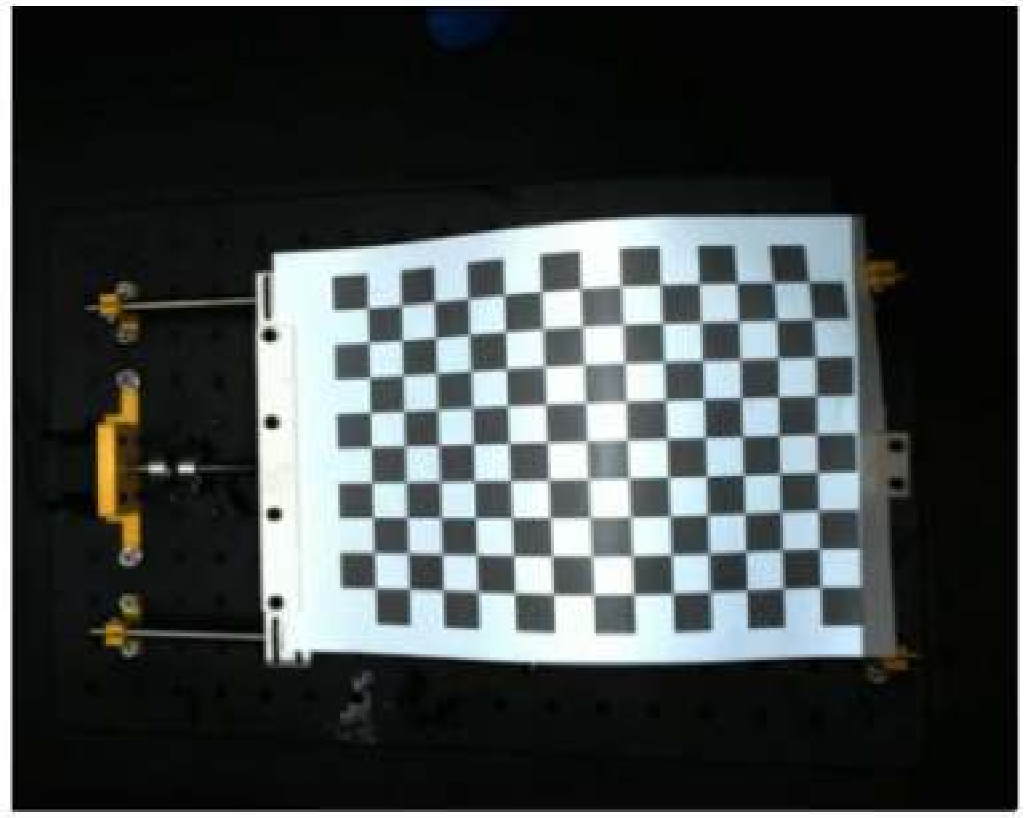

line

circle

semi-circle

Dataset: S.H.N. Jensen *et al*. arXiv.org, 2018.
Applied Method: V. Golyanik *et al*., arXiv.org, 2019.

Related Work

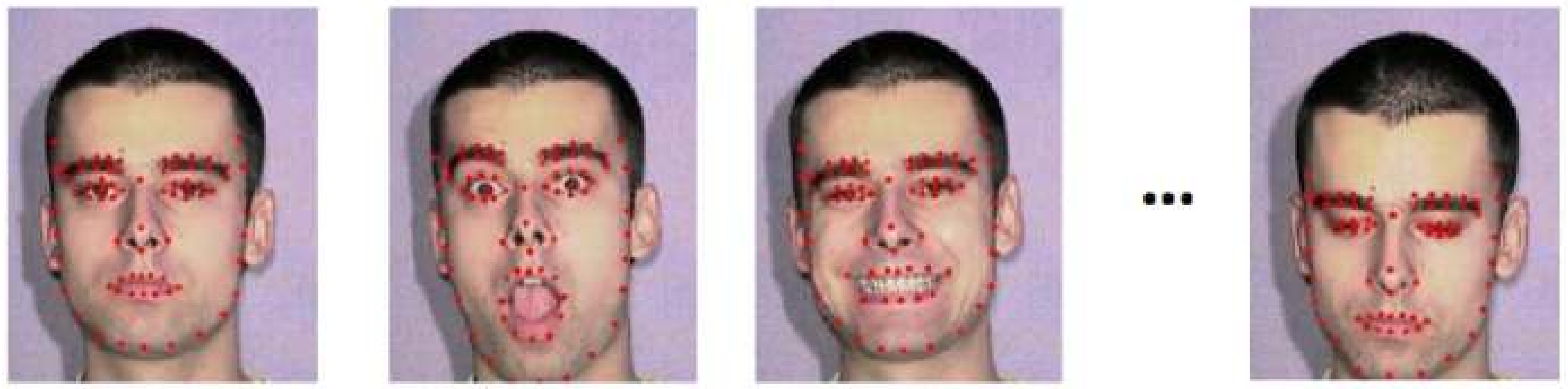

$$\begin{bmatrix} W_1 \\ \vdots \\ W_f \end{bmatrix} = \begin{bmatrix} R_1 & & \\ & \ddots & \\ & & R_f \end{bmatrix} \begin{bmatrix} X_1 \\ \vdots \\ X_f \end{bmatrix}$$

Measurement matrix is known		Camera matrix is unknown		3D shape matrix is unknown
2fn entries	**<**	**6f variables**	**+**	**3fn variables**

[1]

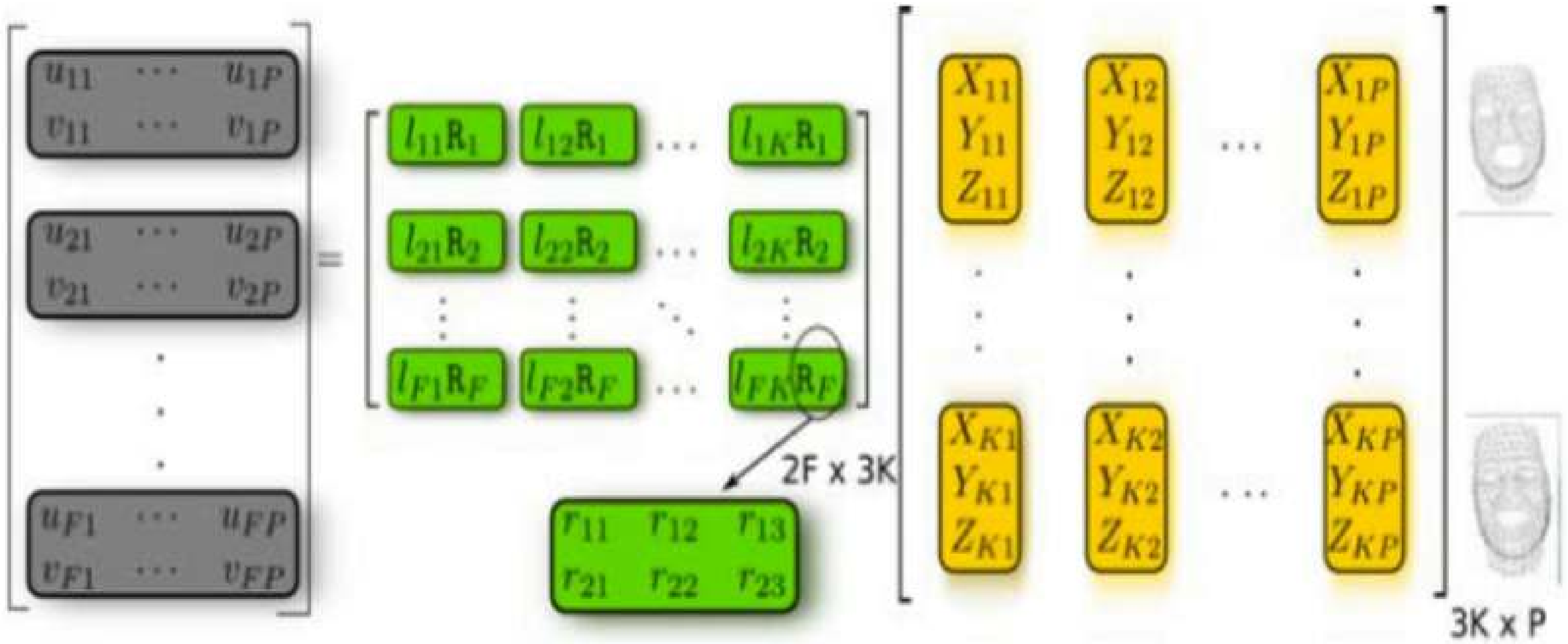

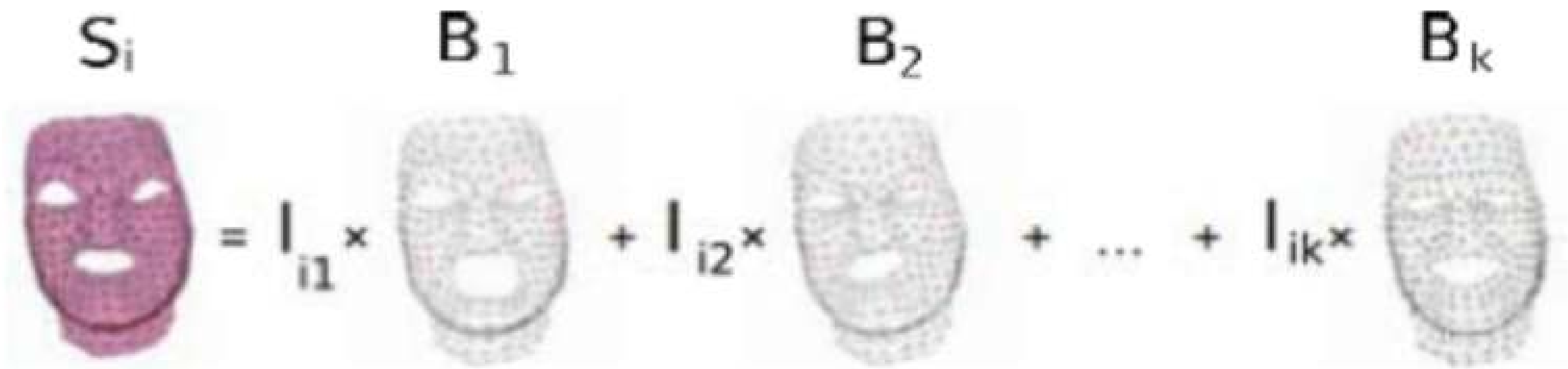

[2]

[1] L. Agapito *et al.*, ICCV 2011 Tutorial on Non-Rigid Registration and Reconstruction.
[2] C. Bregler *et al.*, CVPR, 2000.

Dense NRSfM

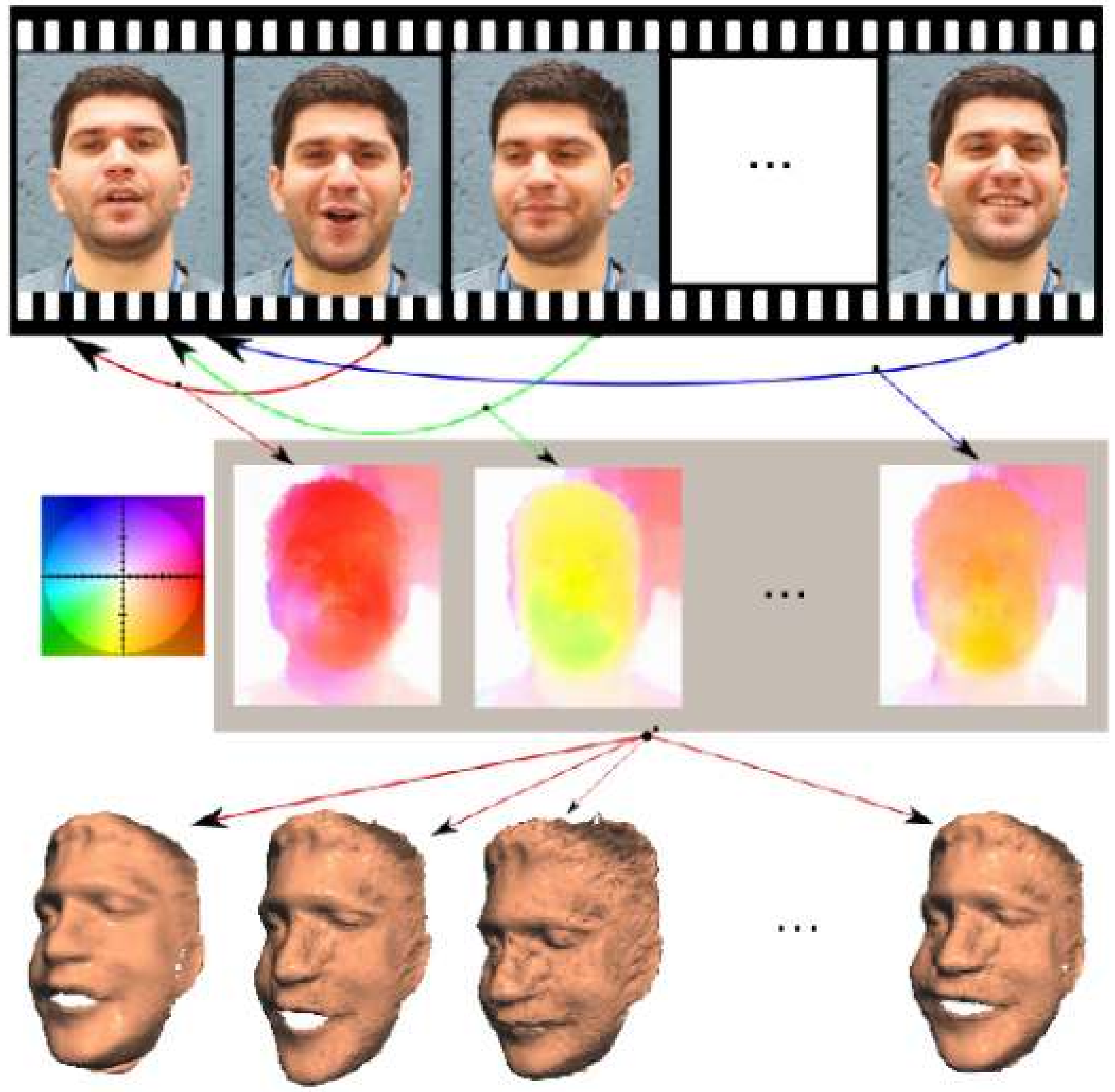

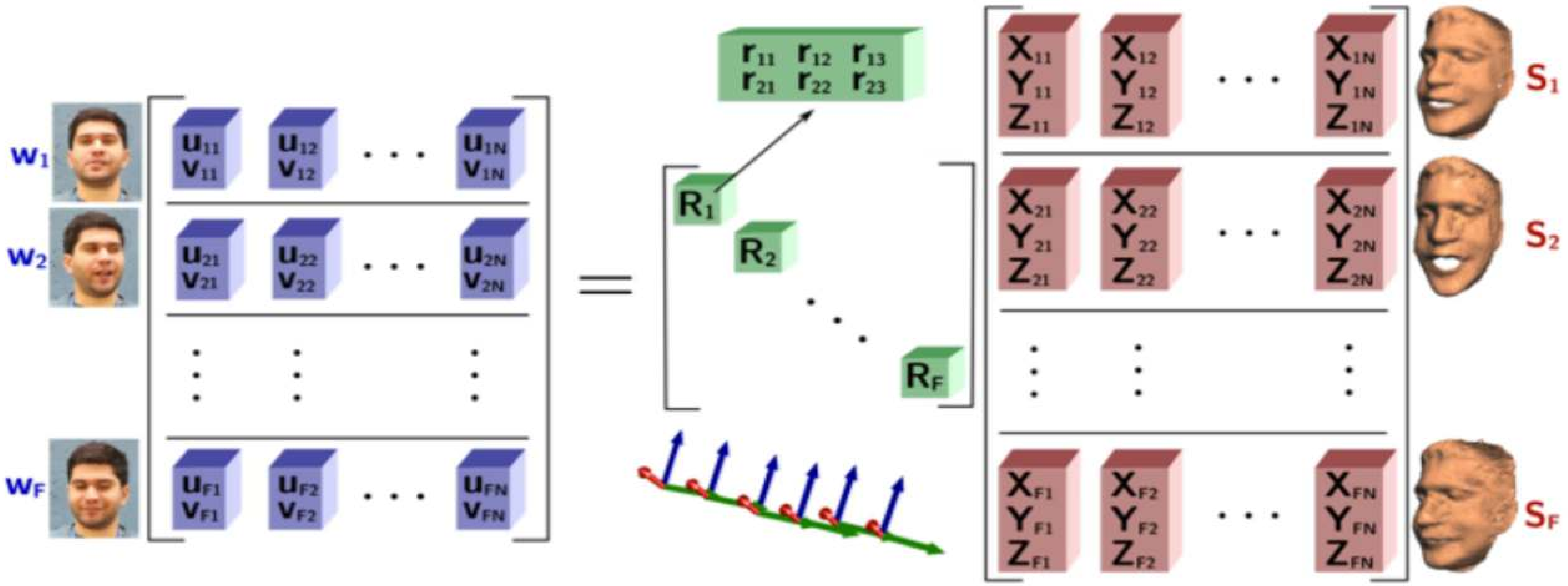

$$\min_{\boldsymbol{S},\boldsymbol{R}} \frac{\lambda}{2}\|\boldsymbol{W}-\boldsymbol{R}\boldsymbol{S}\|_{\mathcal{F}}^2 + \sum_{f,i,p}\|\nabla S_f^i(p)\| + \tau\|P(\boldsymbol{S})\|_*$$

R. Garg *et al.*, CVPR, 2013.

Dense NRSfM

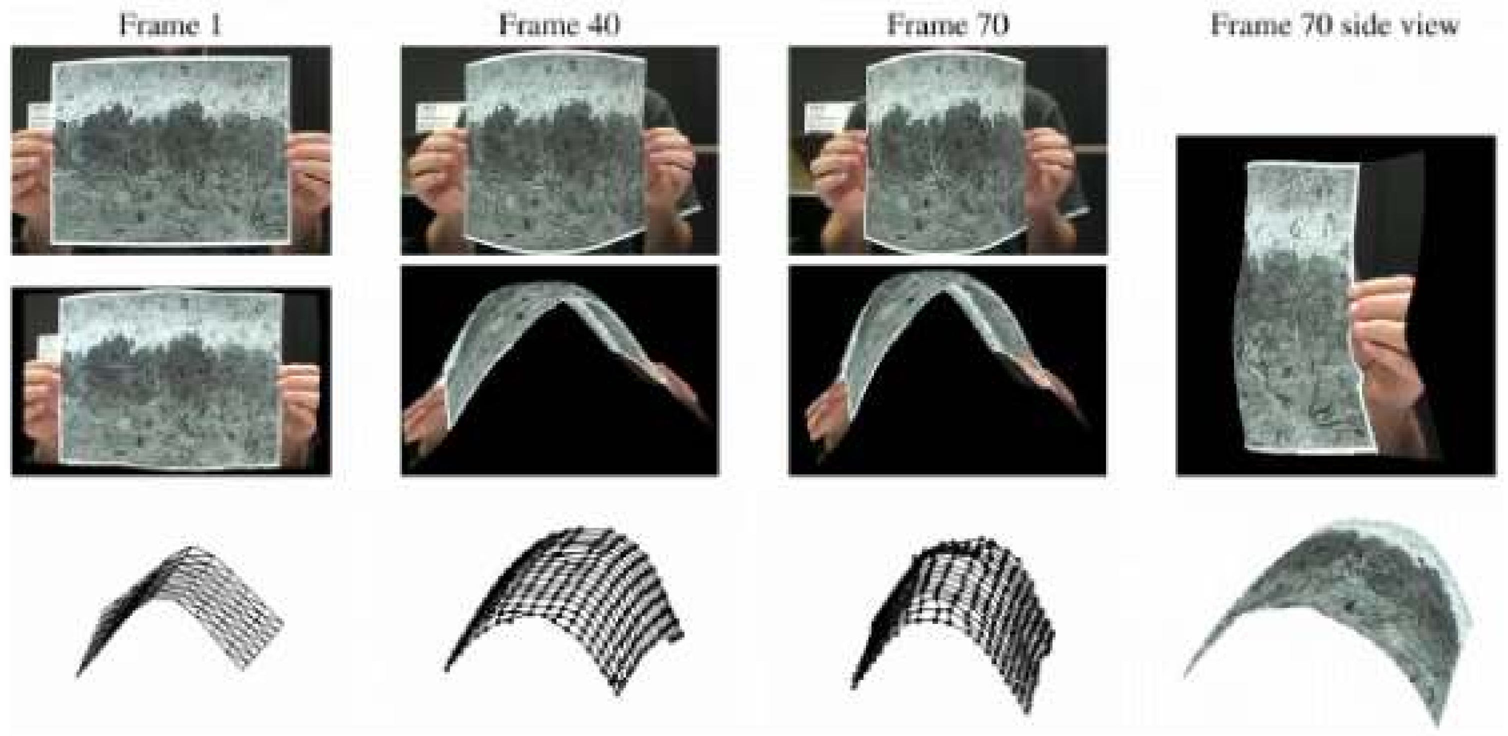

[1]

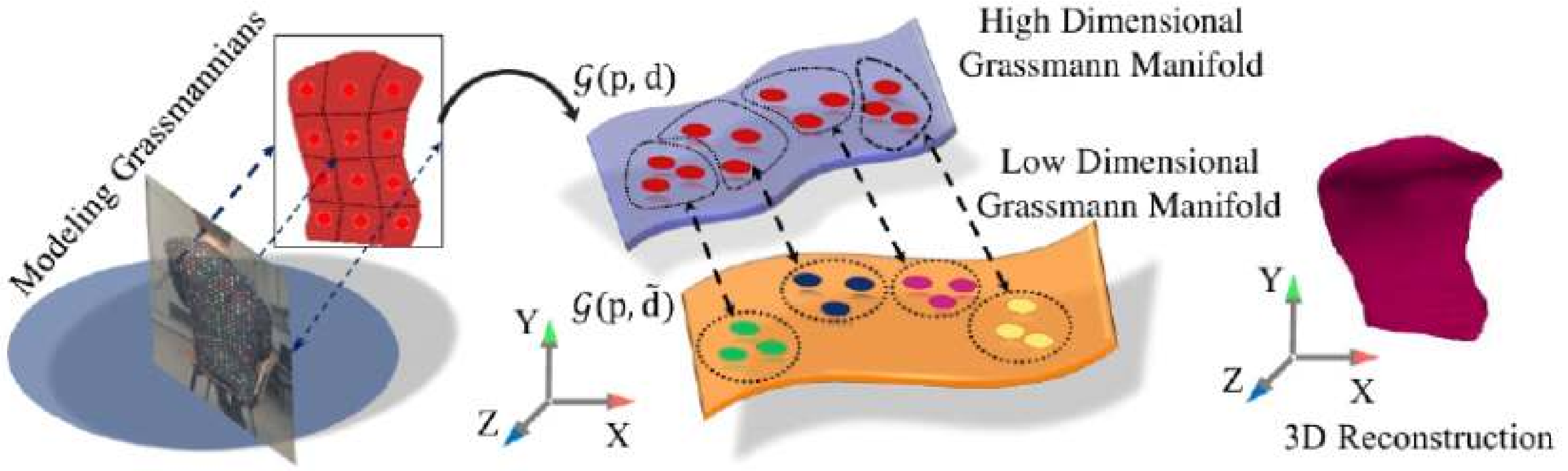

[9]

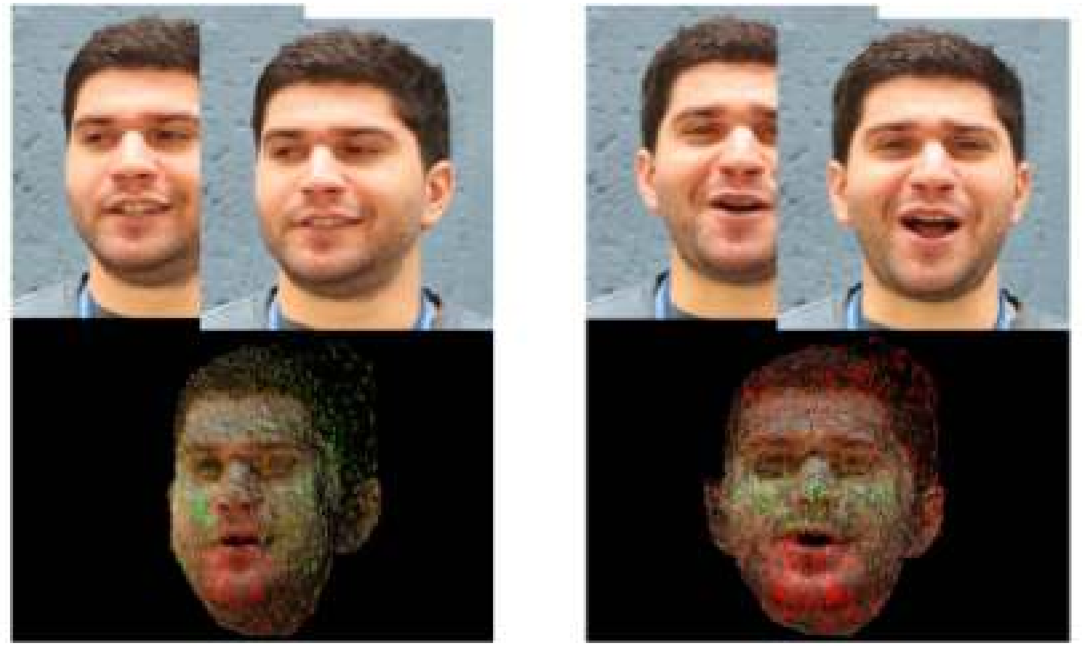

[2]

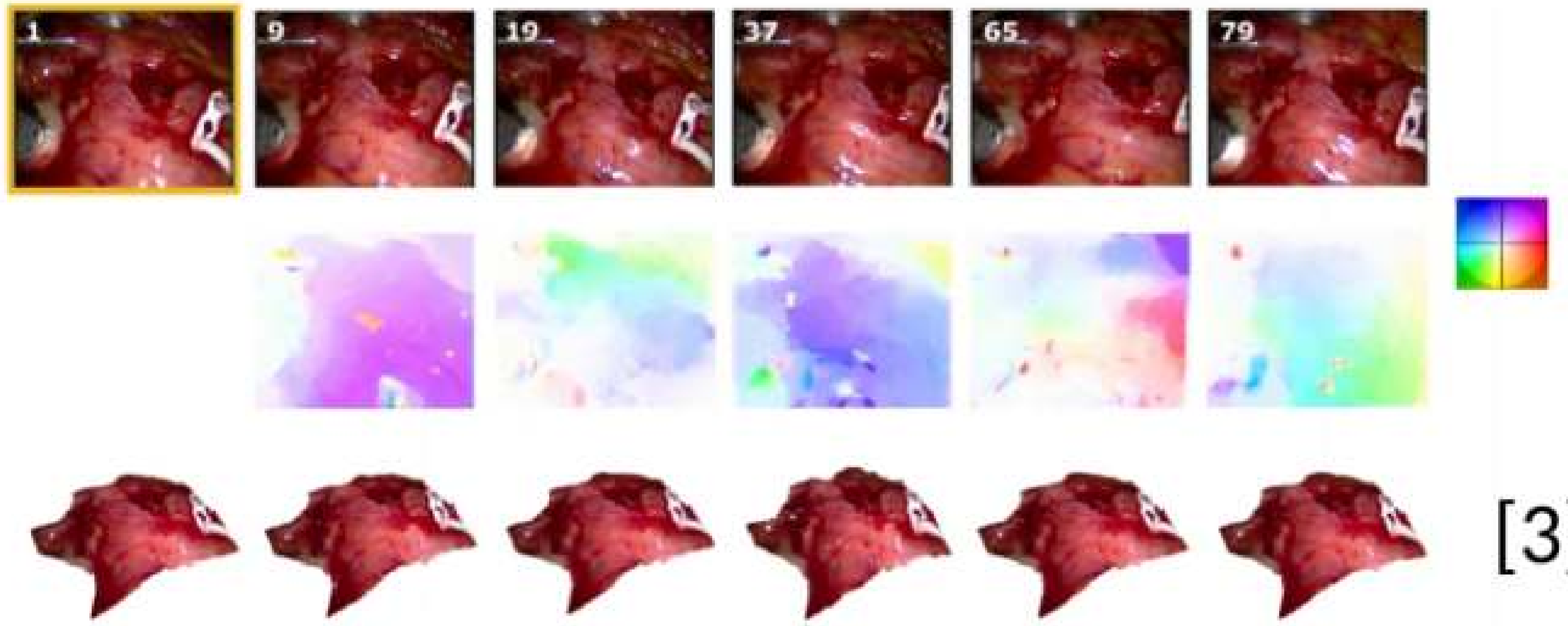

[3]

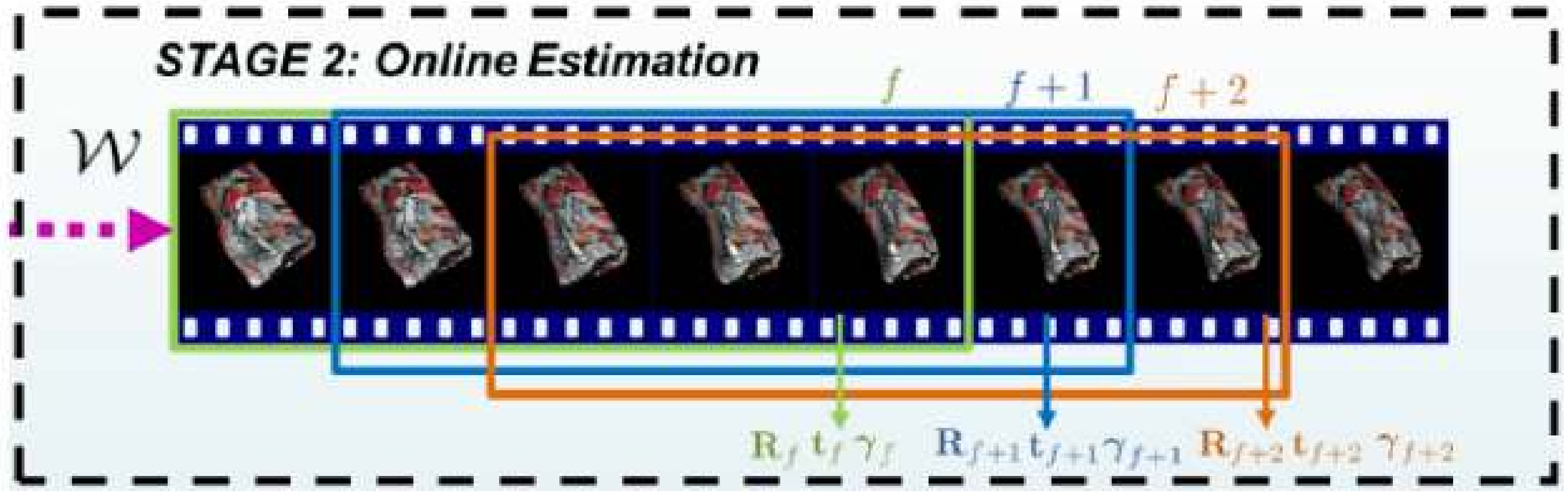

[6]

[1] C. Russel *et al*. Dense Non-rigid Structure from Motion. 3DIMPVT, 2012.
[2] M. D. Ansari *et al*. Scalable Dense Monocular Surface Reconstruction. 3DV, 2017.
[3] V. Golyanik *et al*. Dense Batch Non-Rigid Structure from Motion in a Second. WACV, 2017.
[4] V. Golyanik *et al*. Introduction to Coherent Depth Fields for Dense Monocular Surface Recovery. BMVC, 2017.
[5] V. Golyanik *et al*. Consolidating Segmentwise Non-Rigid Structure from Motion. MVA, 2019.
[6] A. Agudo *et al*., Online Dense Non-Rigid 3D Shape and Camera Motion Recovery. BMVC, 2014.
[7] A. Agudo and F. Moreno-Noguer. A Scalable, Efficient, and Accurate Solution to Non-Rigid Structure from Motion. CVIU, 2018.
[8] S. Kumar *et al*. Scalable Dense Non-rigid Structure-from-Motion: A Grassmannian Perspective. CVPR, 2018.
[9] S. Kumar. Jumping Manifolds: Geometry Aware Dense Non-Rigid Structure from Motion. In CVPR, 2019.

Lifting AutoEncoders

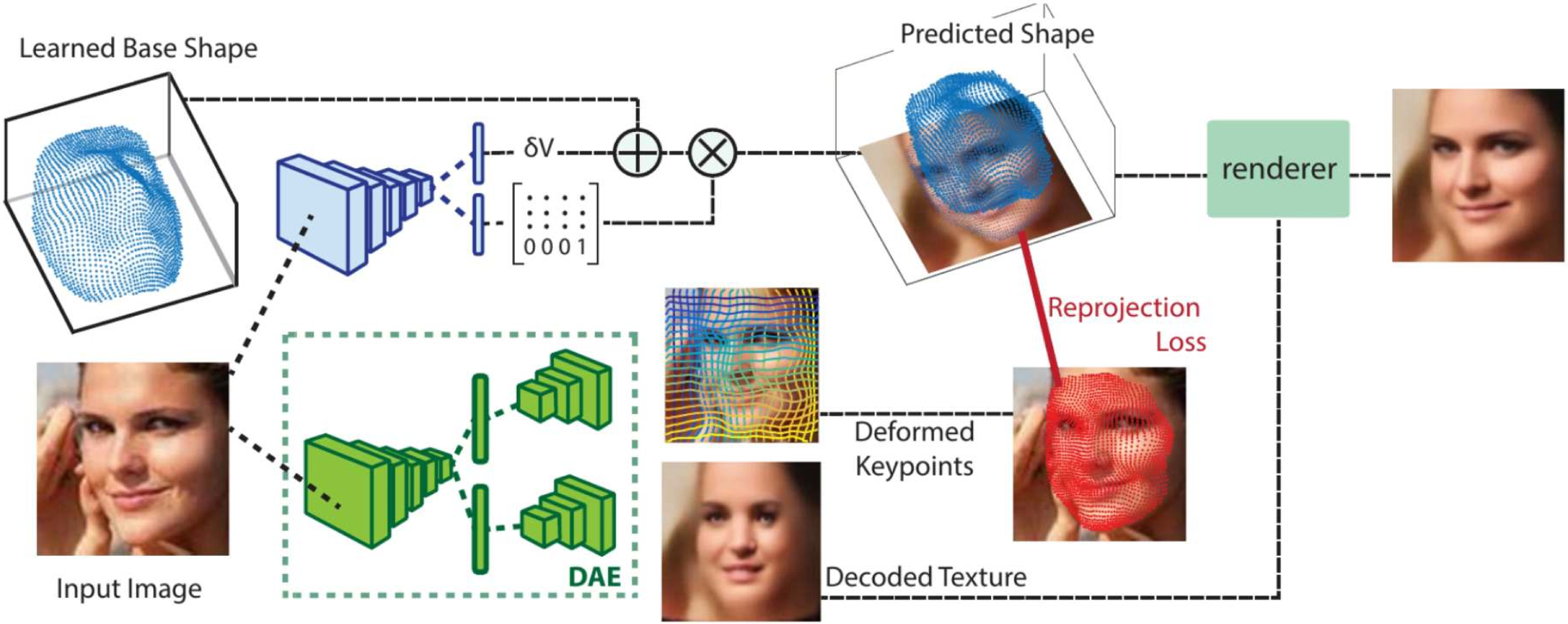

M. Sahasrabudhe and Z. Shu *et al.* ICCV Workshops, 2019.

C3DPO

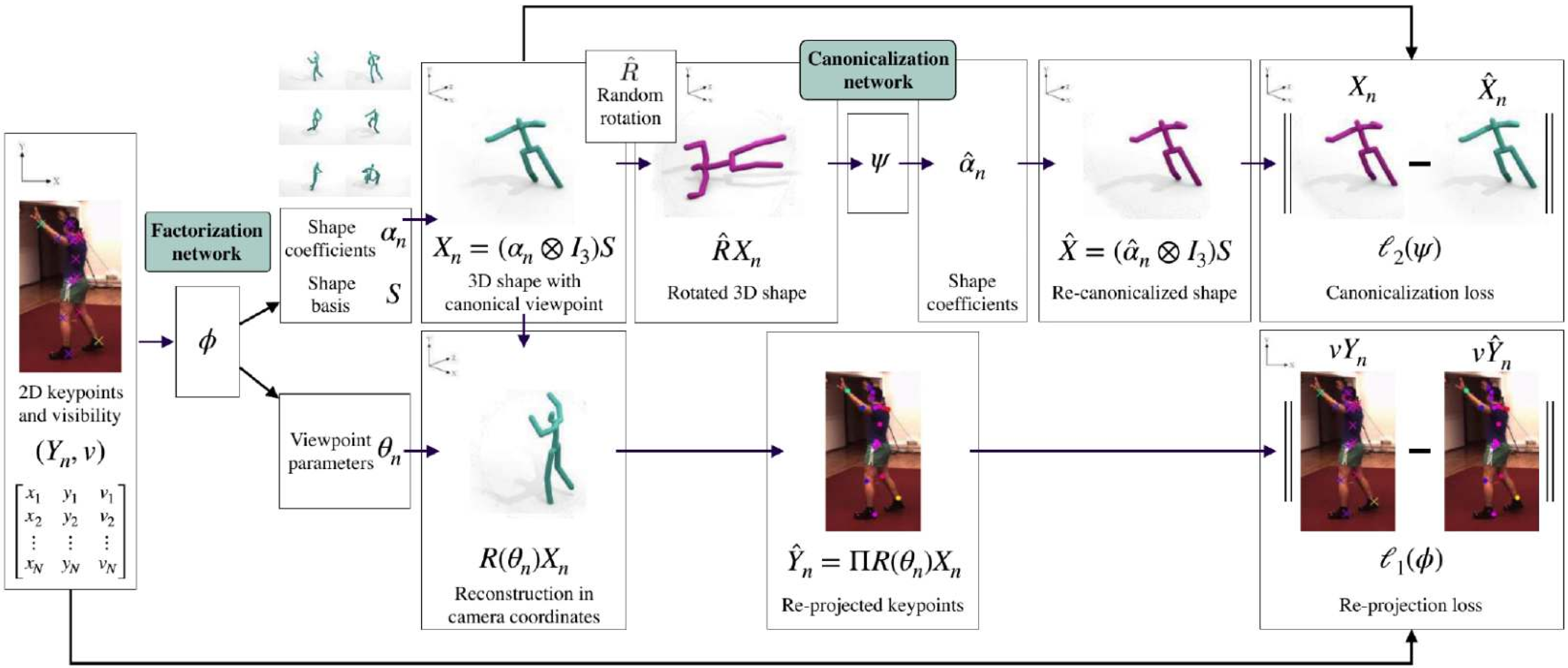

D. Novotny and N. Ravi *et al.* ICCV, 2019.

C3DPO

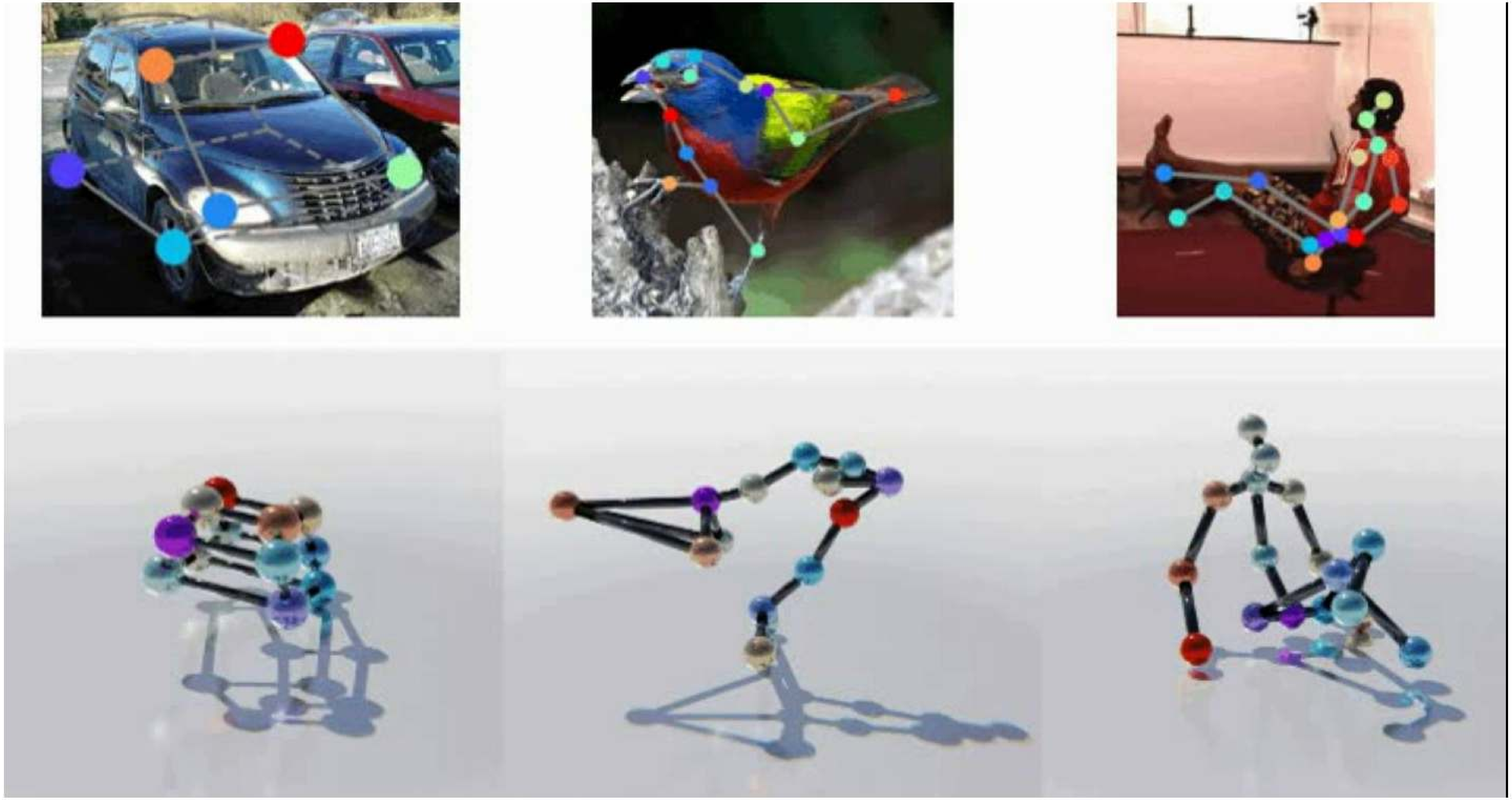

D. Novotny and N. Ravi *et al.* ICCV, 2019.

C3DPO

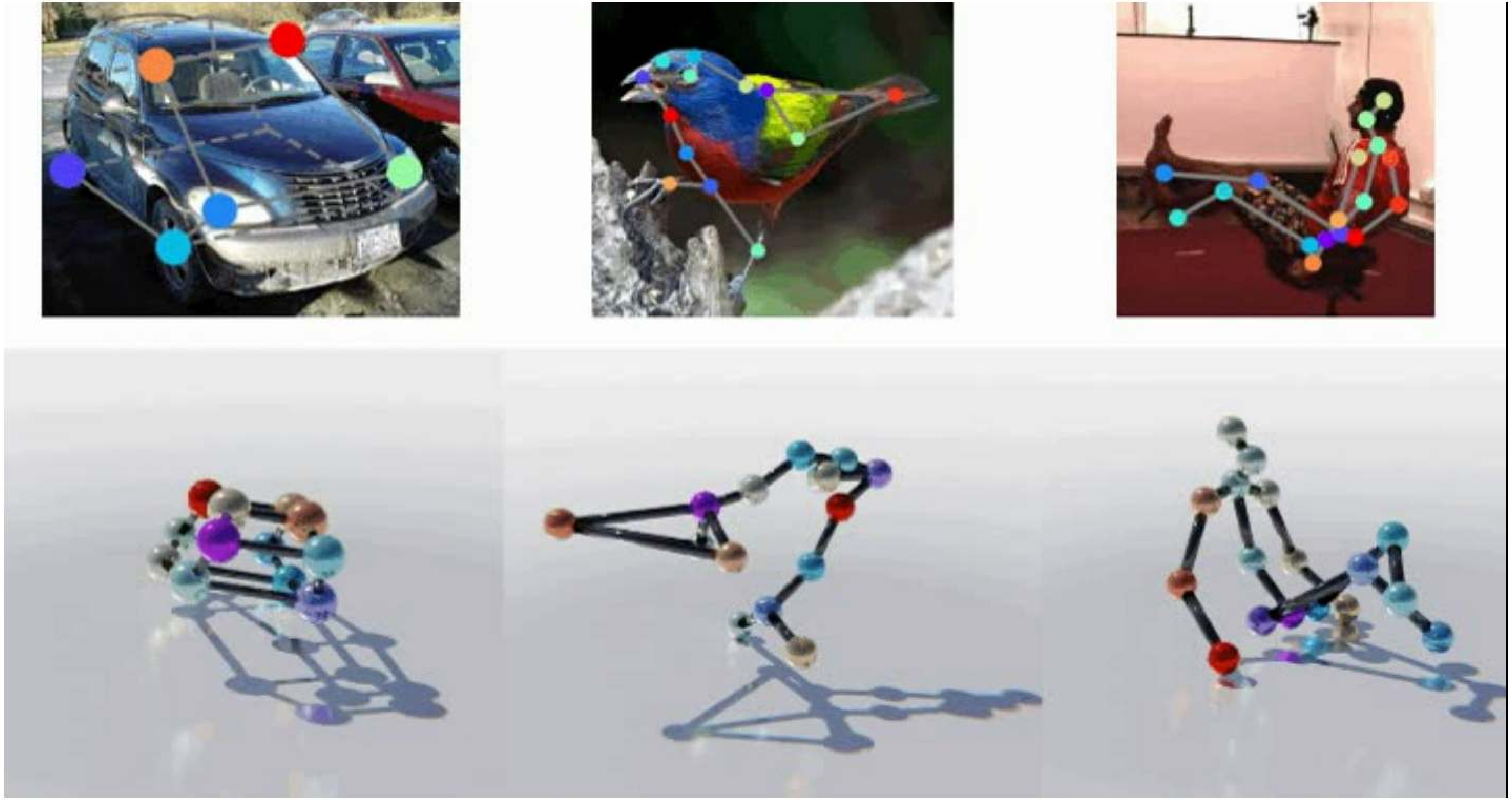

D. Novotny and N. Ravi *et al.* ICCV, 2019.

Deep NRSfM

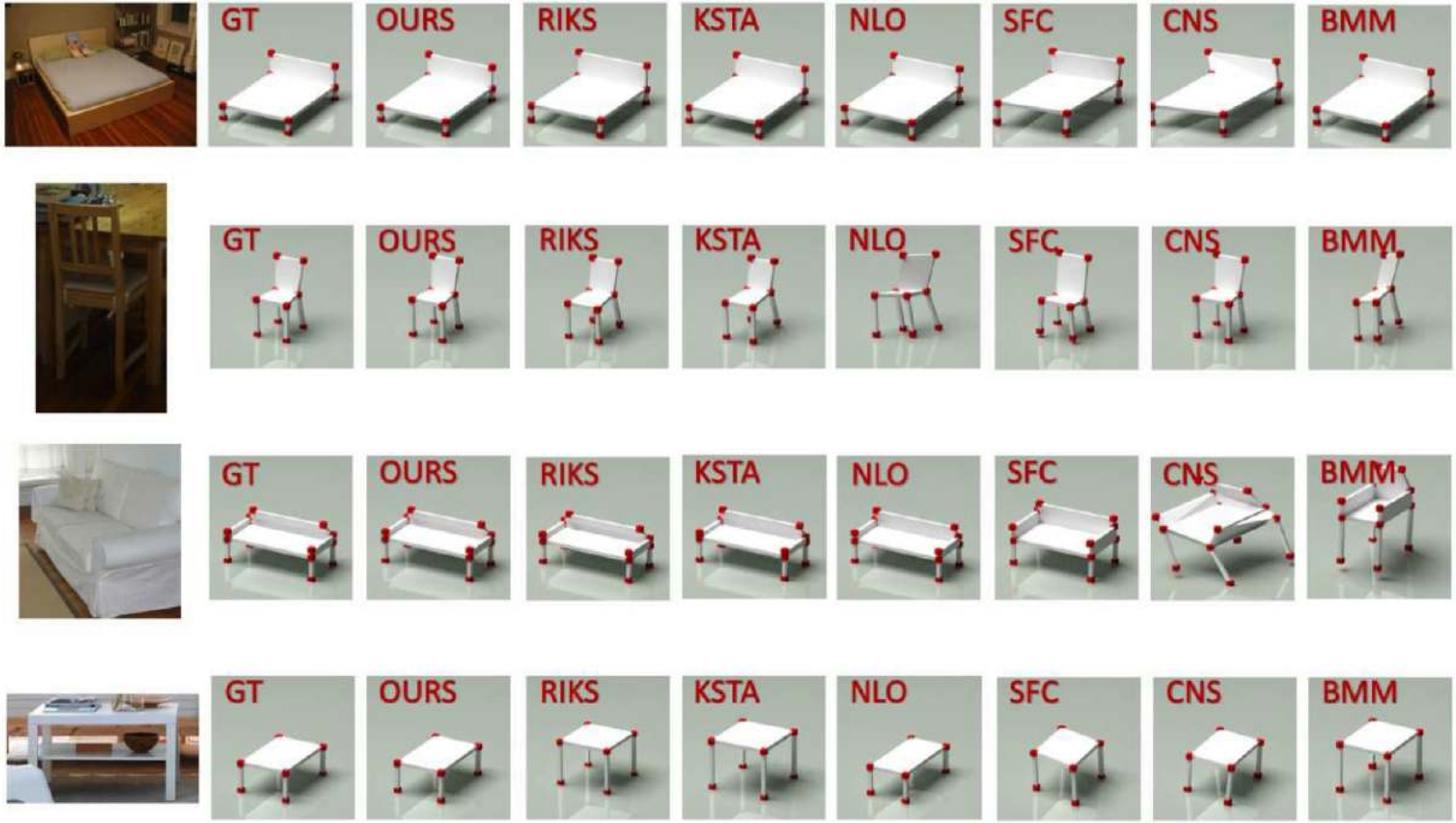

C. Kong and S. Lucey. ICCV, 2019.

Related Work

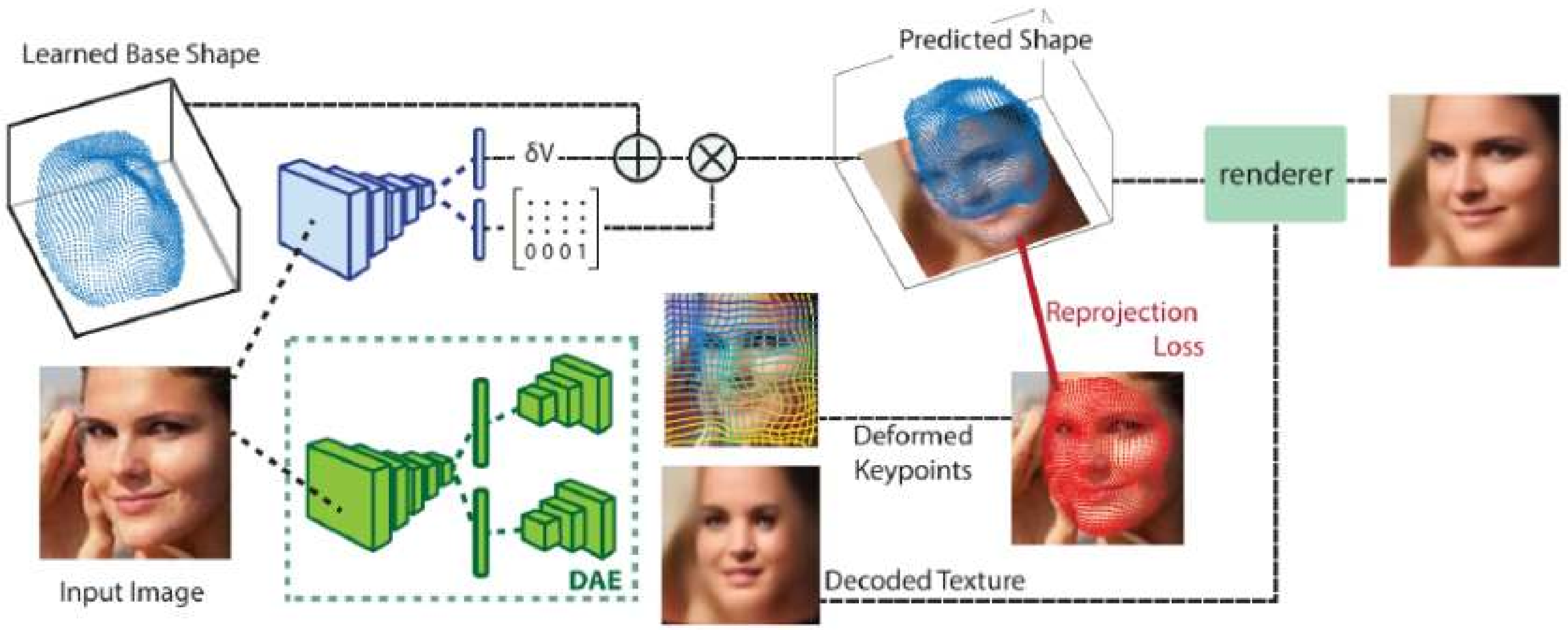

M. Sahasrabudhe and Z. Shu *et al.* ICCV Workshops, 2019.

C. Kong and S. Lucey. ICCV, 2019.

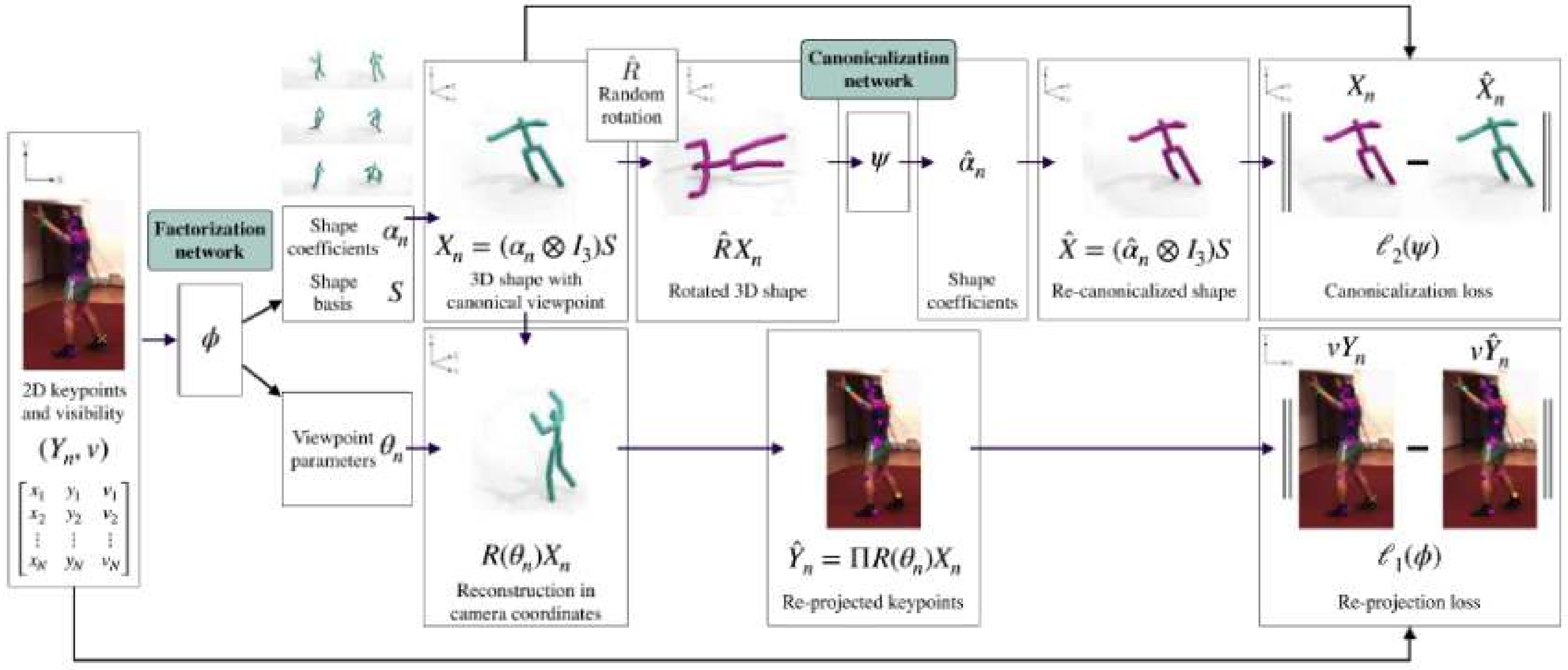

D. Novotny and N. Ravi *et al.* ICCV, 2019.

Our Neural Dense NRSfM

- N-NRSfM does not require 3D supervision and does not rely on annotated 2D data collections
- Core contribution: a new neural deformation model component
- Shapes are recovered during the network training through backpropagation

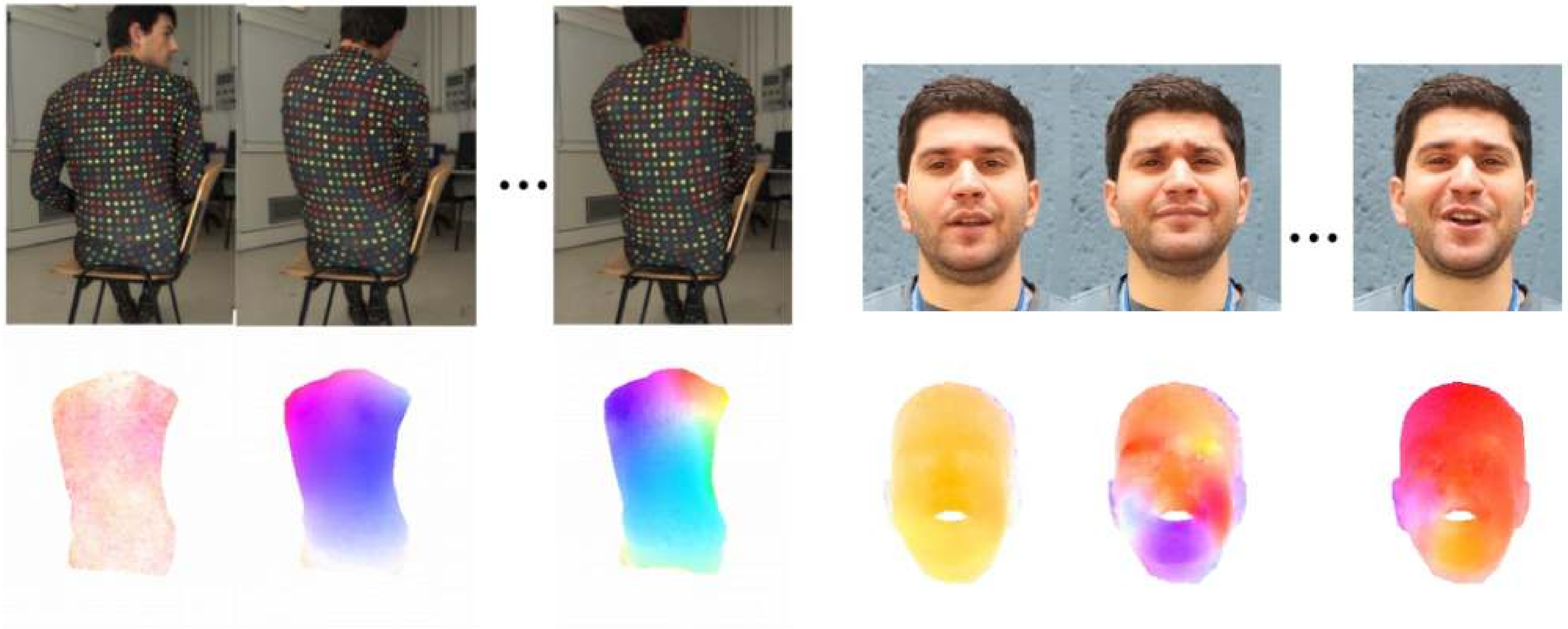

Our Neural Dense NRSfM

- N-NRSfM does not require 3D supervision and does not rely on annotated 2D data collections
- <u>Core contribution</u>: a new neural deformation model component
- Shapes are recovered during the network training through backpropagation

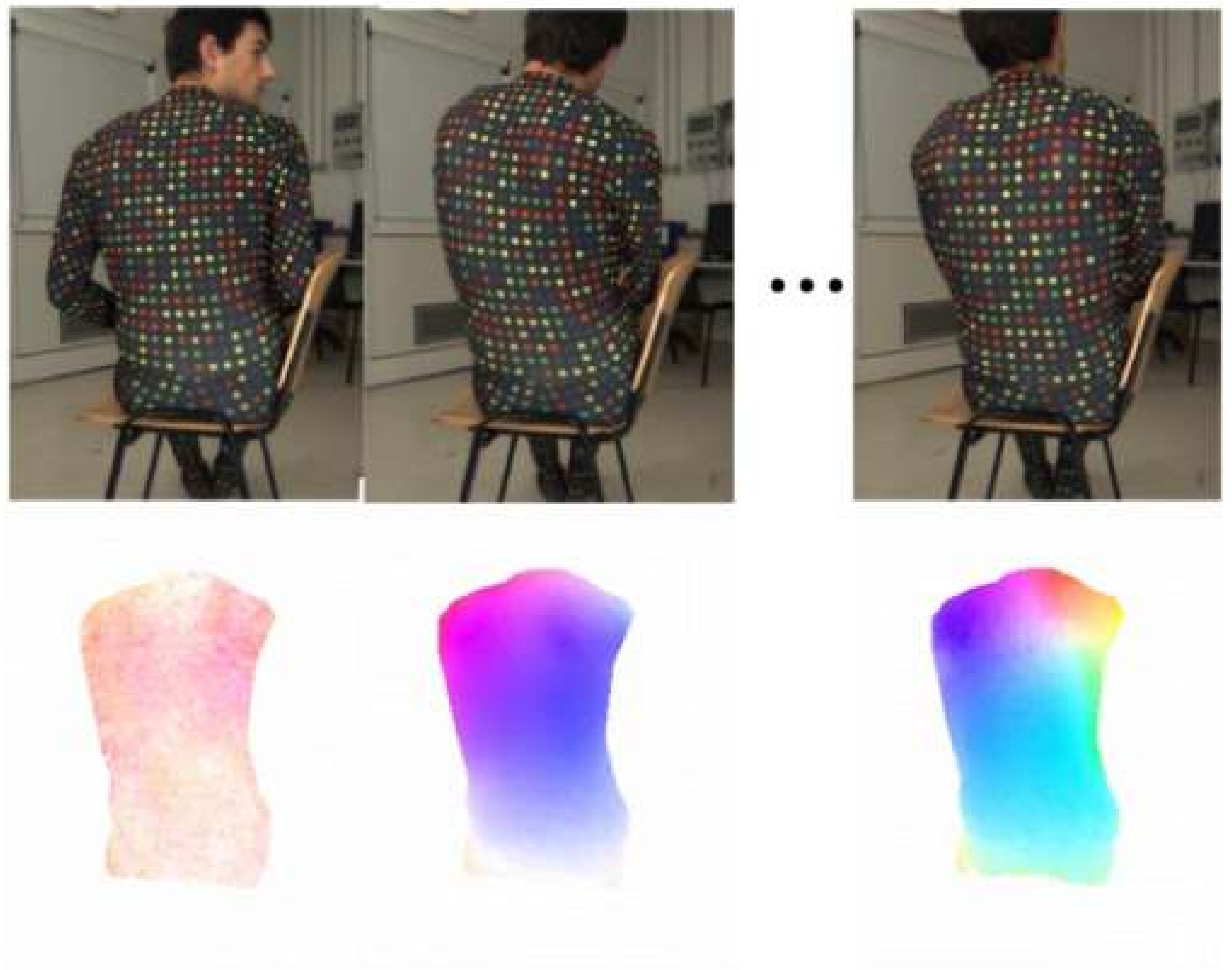

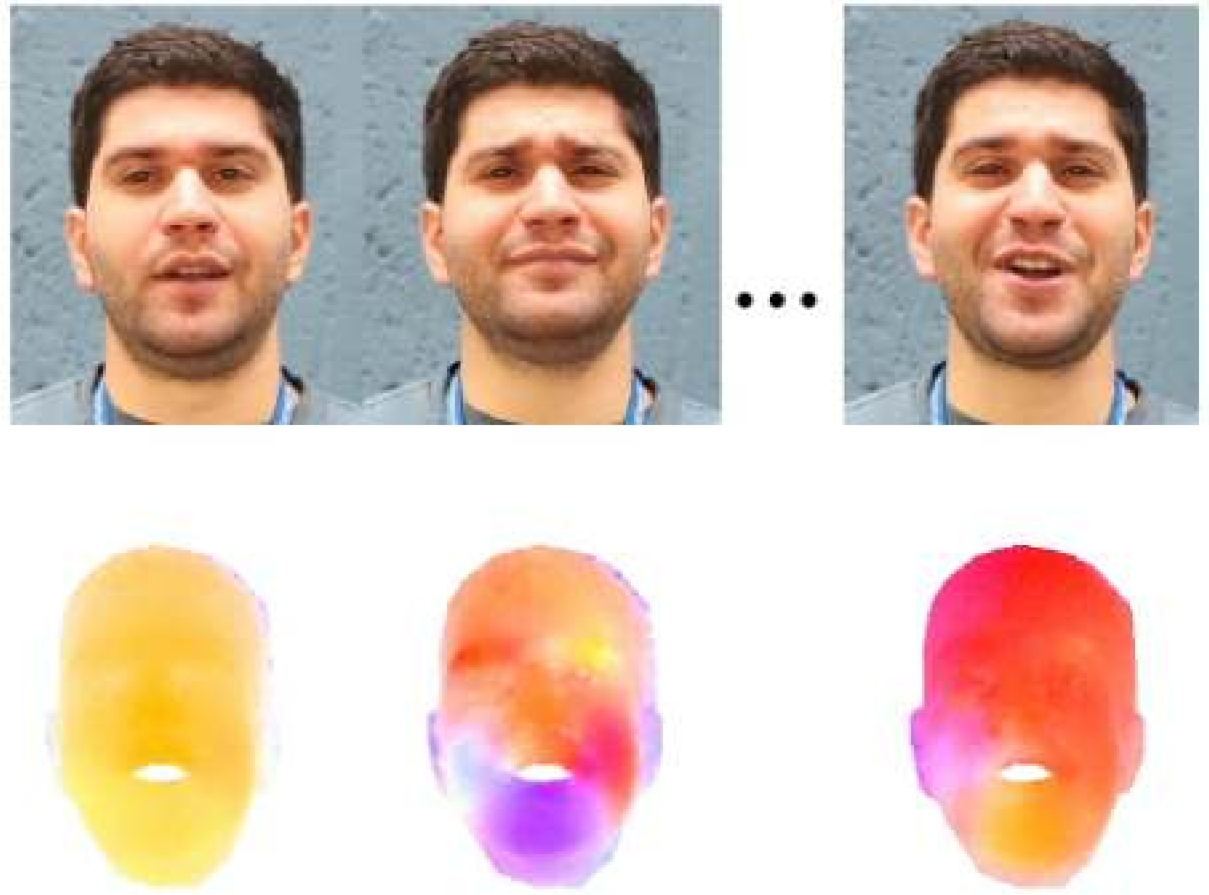

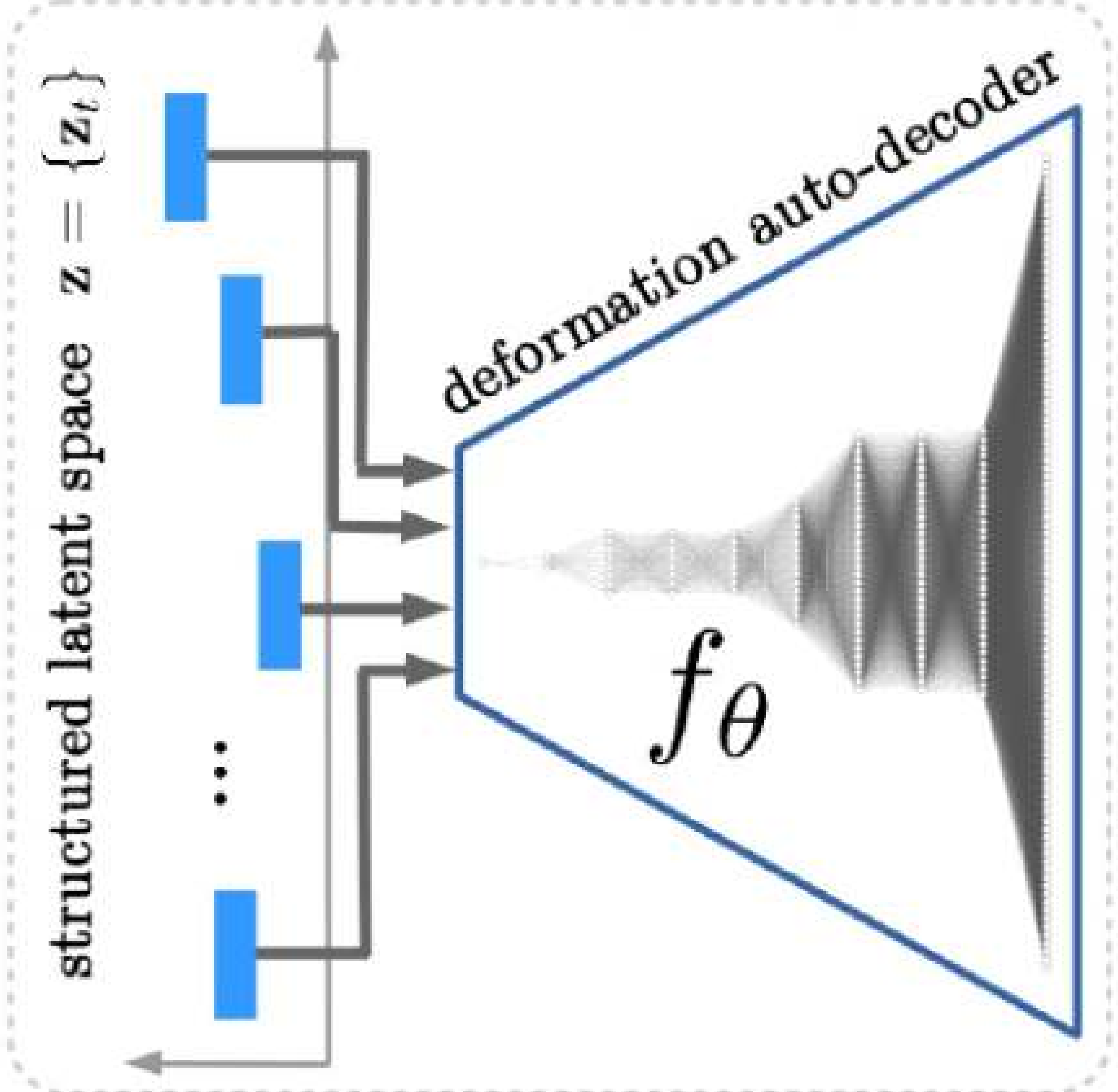

$$\frac{\partial \mathbf{E}}{\partial \boldsymbol{\theta}} = \sum_{t=1}^{T} \frac{\partial \mathbf{E}}{\partial \mathbf{S}_t} \frac{\partial \mathbf{S}_t}{\partial \boldsymbol{\theta}}$$

Method Overview

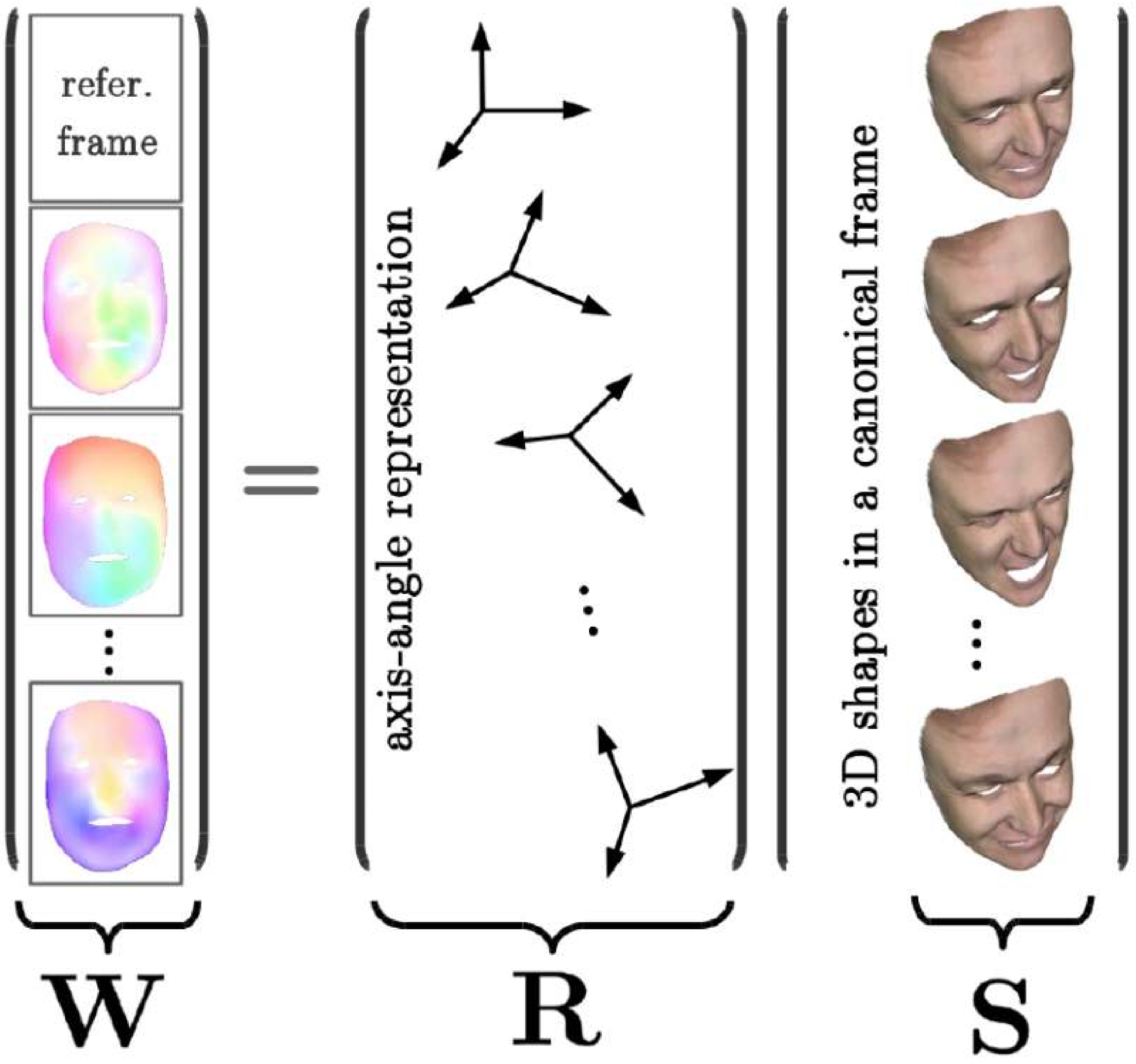

Method Overview

Method Overview

Method Overview

Method Overview

Method Overview

Our Differentiable Energy Function

$$\mathbf{E} = \mathbf{E}_{\text{data}}(\boldsymbol{\theta}, \mathbf{z}, \mathbf{R}) + \beta\,\mathbf{E}_{\text{temp}}(\boldsymbol{\theta}, \mathbf{z}) + \gamma\,\mathbf{E}_{\text{spat}}(\boldsymbol{\theta}, \mathbf{z}) + \eta\,\mathbf{E}_{\text{traj}}(\boldsymbol{\theta}, \mathbf{z}) + \omega\,\mathbf{E}_{\text{latent}}(\mathbf{z})$$

$\boldsymbol{\theta}$ denotes learned network parameters

$\mathbf{z}$ is the latent space function

$f_{\boldsymbol{\theta}}(\mathbf{z})$ are displacements from the mean shape

$\mathbf{R}$ is a block-diagonal matrix of truncated camera rotations

$\beta, \gamma, \eta, \omega$ are the weights balancing the terms

Our Differentiable Energy Function

$$\mathbf{E} = \mathbf{E}_{\text{data}}(\boldsymbol{\theta}, \mathbf{z}, \mathbf{R}) + \beta\, \mathbf{E}_{\text{temp}}(\boldsymbol{\theta}, \mathbf{z}) + \gamma\, \mathbf{E}_{\text{spat}}(\boldsymbol{\theta}, \mathbf{z}) + \eta\, \mathbf{E}_{\text{traj}}(\boldsymbol{\theta}, \mathbf{z}) + \omega\, \mathbf{E}_{\text{latent}}(\mathbf{z})$$

$\boldsymbol{\theta}$ denotes learned network parameters

$\mathbf{z}$ is the latent space function

$f_{\boldsymbol{\theta}}(\mathbf{z})$ are displacements from the mean shape

$\mathbf{R}$ is a block-diagonal matrix of truncated camera rotations

$\beta, \gamma, \eta, \omega$ are the weights balancing the terms

$$\mathbf{S}_t = \bar{\mathbf{S}} + f_{\boldsymbol{\theta}}(\mathbf{z}_t)$$

Our Differentiable Energy Function

$$\mathbf{E} = \mathbf{E}_{\text{data}}(\boldsymbol{\theta}, \mathbf{z}, \mathbf{R}) + \beta\, \mathbf{E}_{\text{temp}}(\boldsymbol{\theta}, \mathbf{z}) + \gamma\, \mathbf{E}_{\text{spat}}(\boldsymbol{\theta}, \mathbf{z}) + \eta\, \mathbf{E}_{\text{traj}}(\boldsymbol{\theta}, \mathbf{z}) + \omega\, \mathbf{E}_{\text{latent}}(\mathbf{z})$$

$\boldsymbol{\theta}$ denotes learned network parameters

$\mathbf{z}$ is the latent space function

$f_{\boldsymbol{\theta}}(\mathbf{z})$ are displacements from the mean shape

$\mathbf{R}$ is a block-diagonal matrix of truncated camera rotations

$\beta, \gamma, \eta, \omega$ are the weights balancing the terms

$$\mathbf{S}_t = \bar{\mathbf{S}} + f_{\boldsymbol{\theta}}(\mathbf{z}_t)$$

$$\boxed{\frac{\partial \mathbf{E}}{\partial \boldsymbol{\theta}} = \sum_{t=1}^{T} \frac{\partial \mathbf{E}}{\partial \mathbf{S}_t} \frac{\partial \mathbf{S}_t}{\partial \boldsymbol{\theta}}}$$

Our Differentiable Energy Function

$$\mathbf{E} = \mathbf{E}_{\text{data}}(\boldsymbol{\theta}, \mathbf{z}, \mathbf{R}) + \beta\, \mathbf{E}_{\text{temp}}(\boldsymbol{\theta}, \mathbf{z}) + \gamma\, \mathbf{E}_{\text{spat}}(\boldsymbol{\theta}, \mathbf{z}) + \eta\, \mathbf{E}_{\text{traj}}(\boldsymbol{\theta}, \mathbf{z}) + \omega\, \mathbf{E}_{\text{latent}}(\mathbf{z})$$

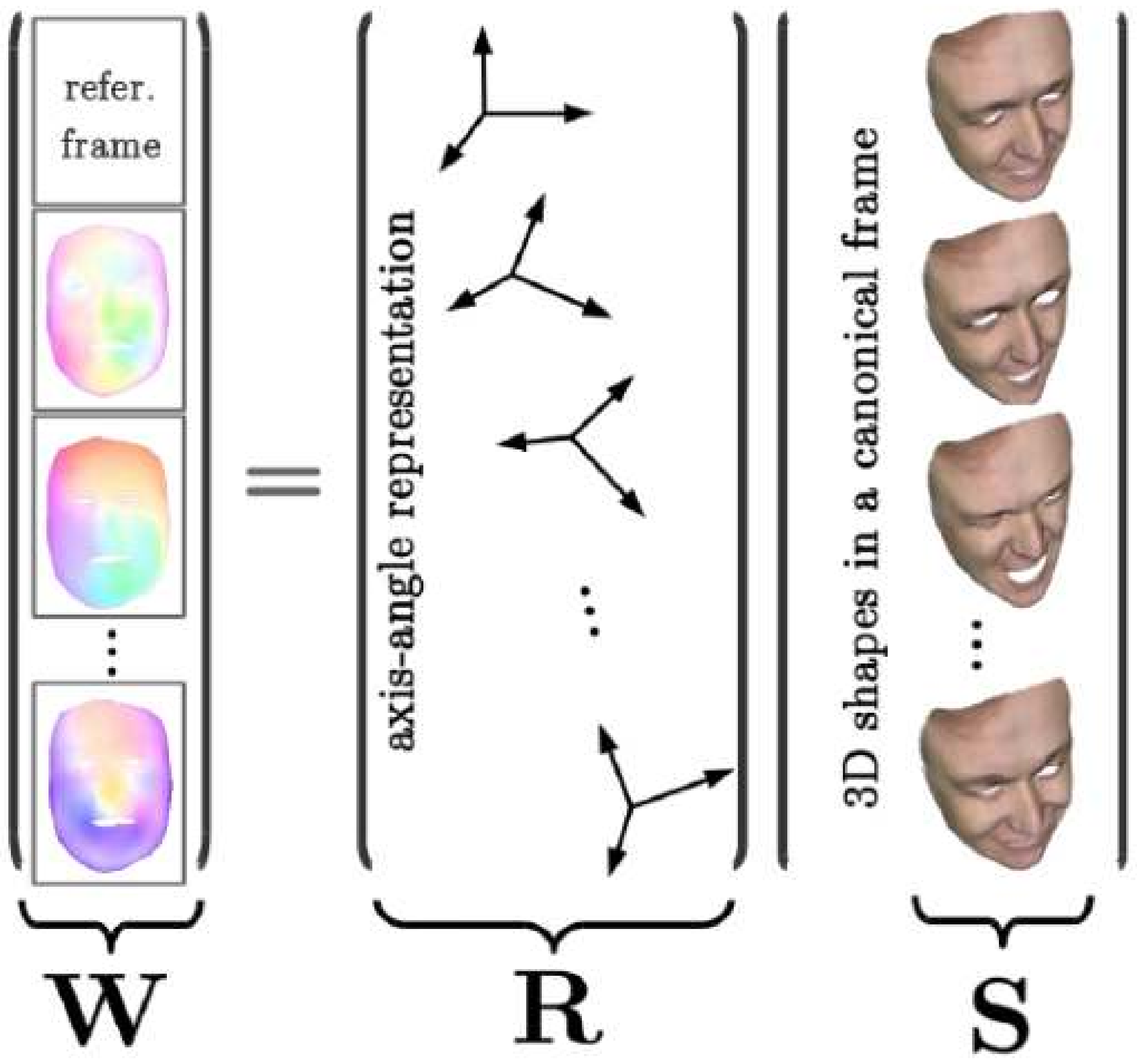

Our Differentiable Energy Function

$$\mathbf{E} = \mathbf{E}_{\text{data}}(\boldsymbol{\theta}, \mathbf{z}, \mathbf{R}) + \beta\, \mathbf{E}_{\text{temp}}(\boldsymbol{\theta}, \mathbf{z}) + \gamma\, \mathbf{E}_{\text{spat}}(\boldsymbol{\theta}, \mathbf{z}) + \eta\, \mathbf{E}_{\text{traj}}(\boldsymbol{\theta}, \mathbf{z}) + \omega\, \mathbf{E}_{\text{latent}}(\mathbf{z})$$

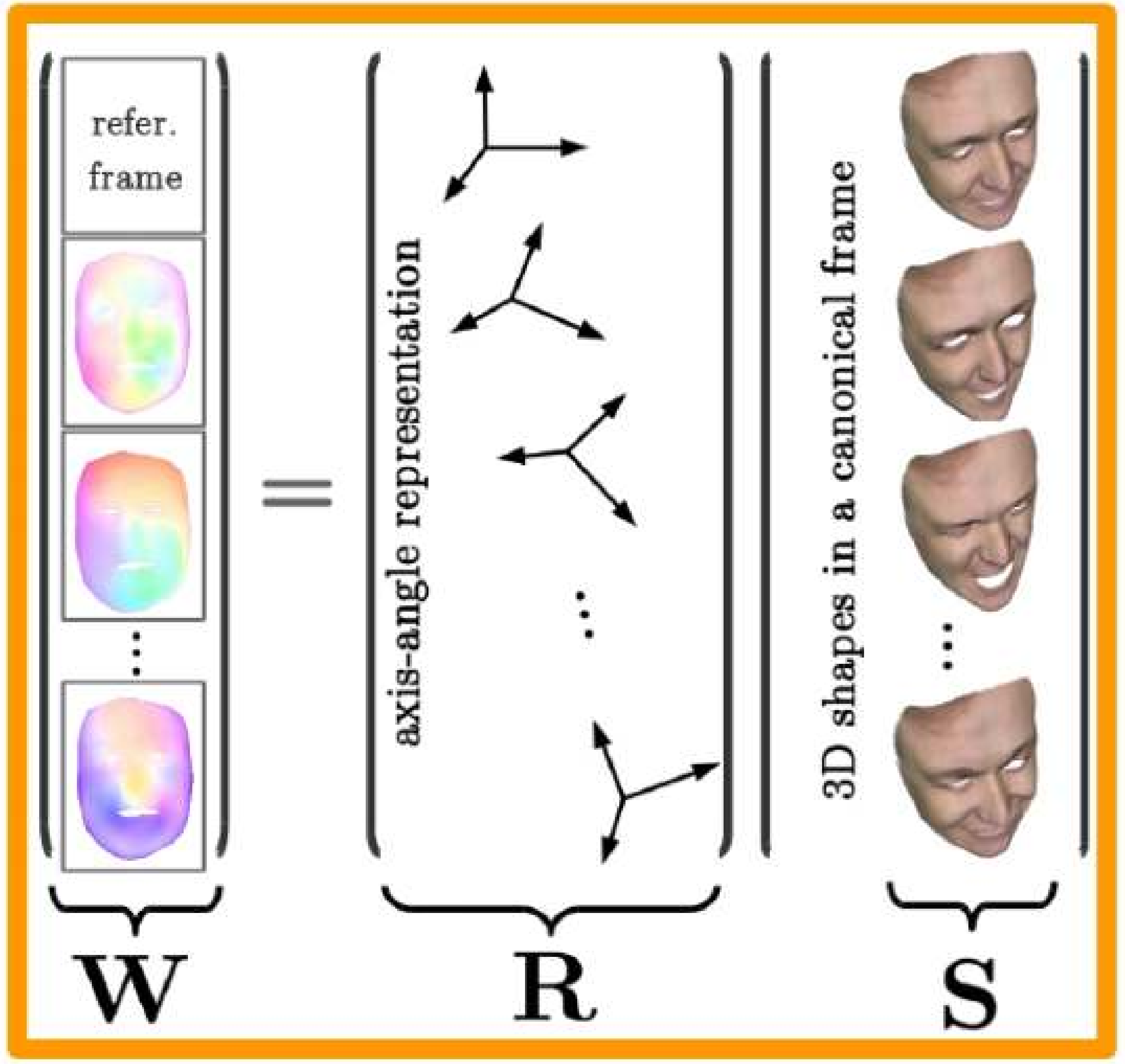

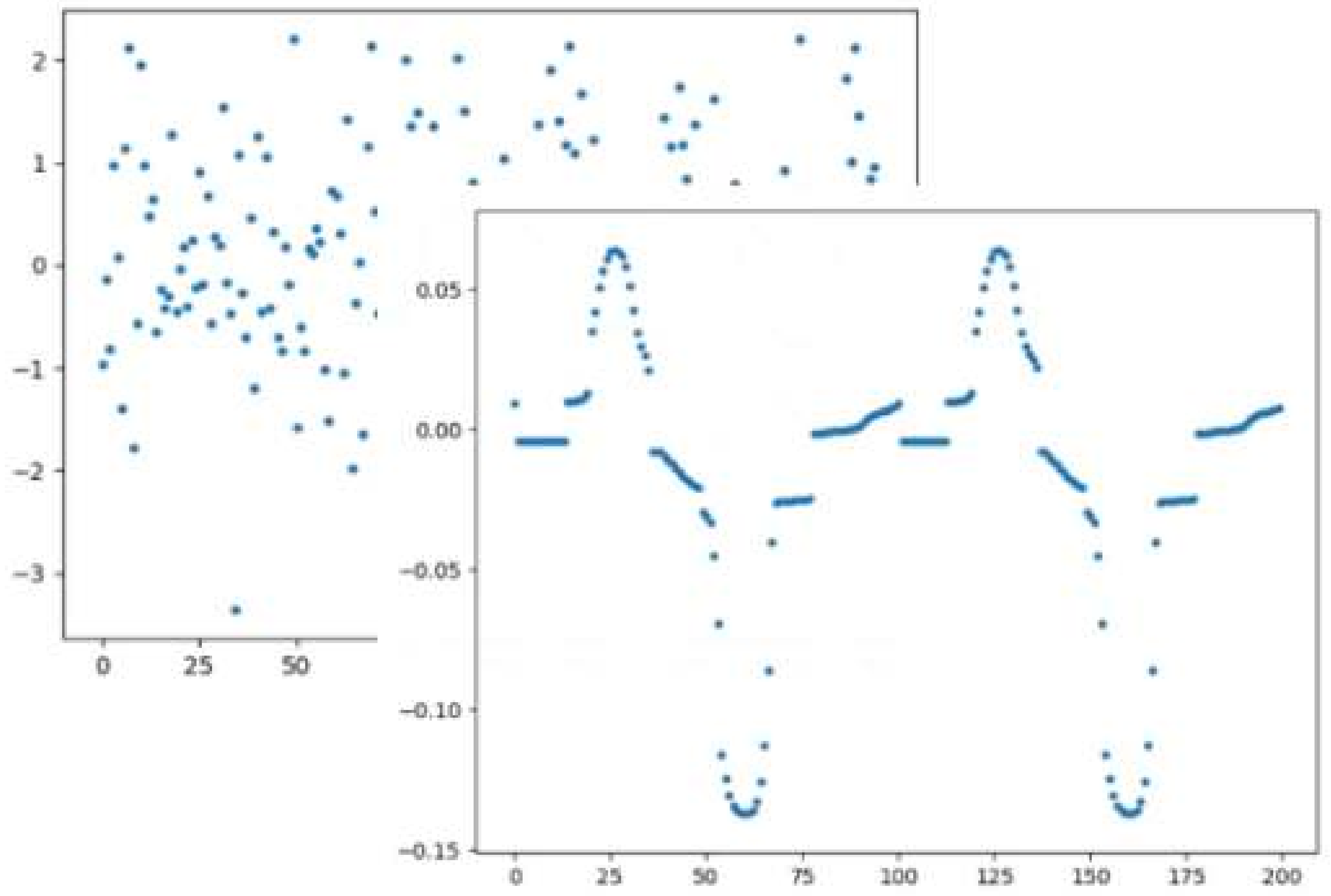

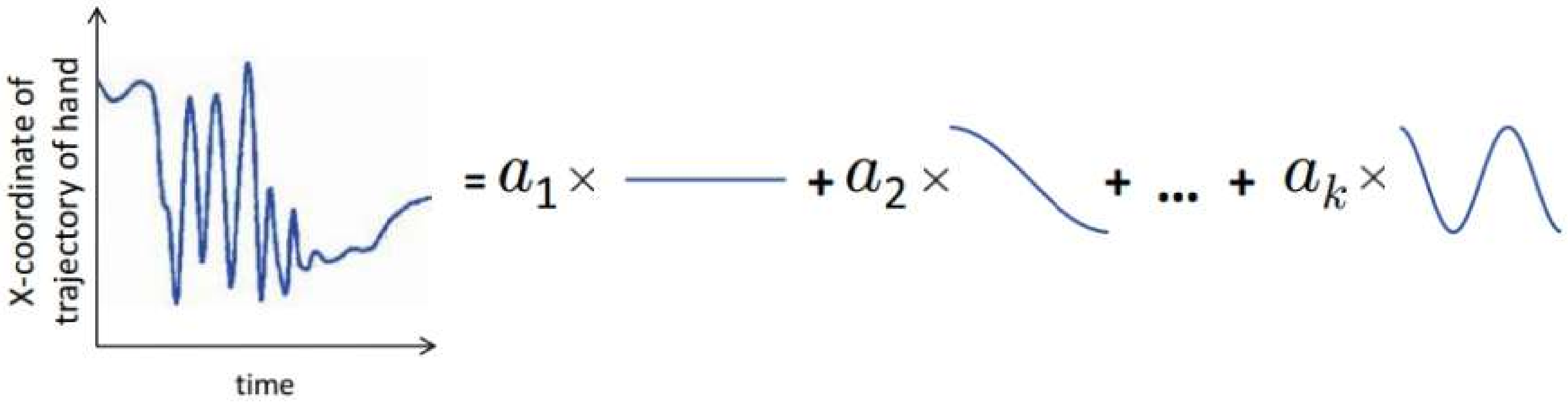

Temporal Regularisation

$$\mathbf{E}_{\text{temp}}(\boldsymbol{\theta}, \mathbf{z}) = \sum_{t=1}^{T-1} \| f_{\boldsymbol{\theta}}(\mathbf{z}_{t+1}) - f_{\boldsymbol{\theta}}(\mathbf{z}_t) \|_{\epsilon}$$

$$\mathbf{E}_{\text{traj}}(\boldsymbol{\theta}, \mathbf{z}) = \left\| (\mathbf{1}_T \otimes \bar{\mathbf{S}}) + f_{\boldsymbol{\theta}}(\mathbf{z}) - (\boldsymbol{\Phi} \otimes \mathbf{I}_3)\mathbf{A} \right\|_{\epsilon}, \quad \boldsymbol{\Phi} = \begin{pmatrix} \phi_{1,1} & \dots & \phi_{1,K} \\ \vdots & \ddots & \vdots \\ \phi_{T,1} & \dots & \phi_{T,K} \end{pmatrix}$$

Temporal Regularisation

$$\mathbf{E}_{\text{temp}}(\boldsymbol{\theta}, \mathbf{z}) = \sum_{t=1}^{T-1} \| f_{\boldsymbol{\theta}}(\mathbf{z}_{t+1}) - f_{\boldsymbol{\theta}}(\mathbf{z}_t) \|_{\epsilon}$$

$$\mathbf{E}_{\text{traj}}(\boldsymbol{\theta}, \mathbf{z}) = \left\| (\mathbf{1}_T \otimes \bar{\mathbf{S}}) + f_{\boldsymbol{\theta}}(\mathbf{z}) - (\boldsymbol{\Phi} \otimes \mathbf{I}_3)\mathbf{A} \right\|_{\epsilon}, \quad \boldsymbol{\Phi} = \begin{pmatrix} \phi_{1,1} & \dots & \phi_{1,K} \\ \vdots & \ddots & \vdots \\ \phi_{T,1} & \dots & \phi_{T,K} \end{pmatrix}$$

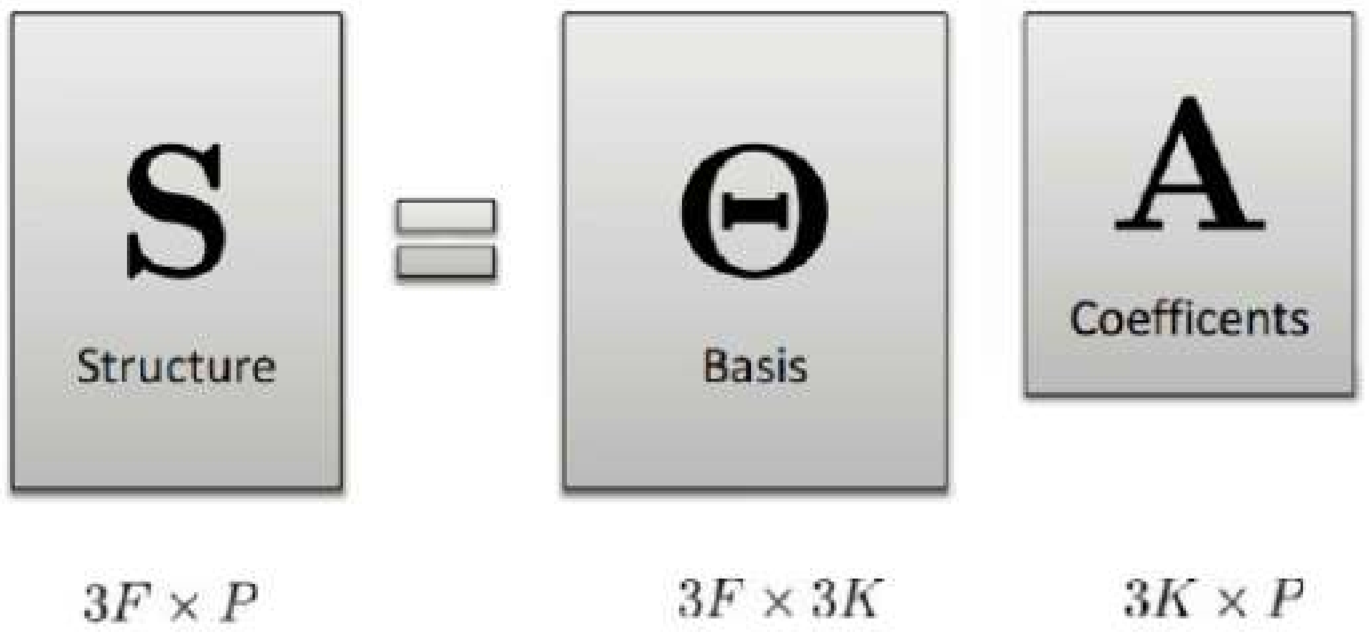

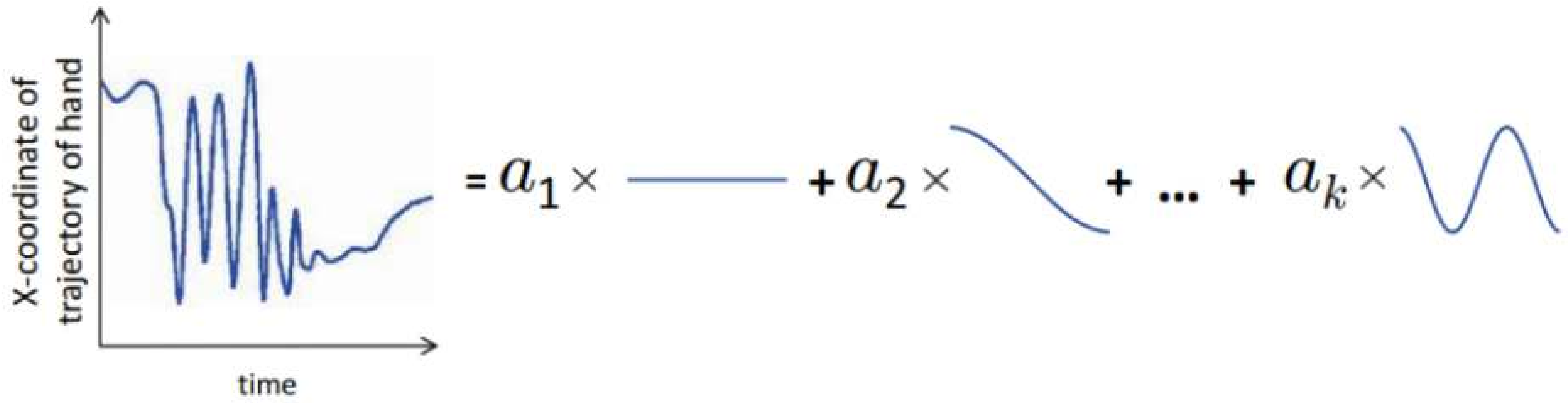

[1]

[1] H. S. Park. 3D reconstruction of a moving point from a series of 2D projections. ECCV, 2010.

Spatial Regulariser

$$\mathbf{E}_{\text{spat}}(\boldsymbol{\theta}, \mathbf{z}) = \underbrace{\sum_{t=0}^{T-1} \sum_{\mathbf{p} \in \mathbf{S}_t} \left\| \mathbf{p} - \frac{1}{|\mathcal{N}(\mathbf{p})|} \sum_{\mathbf{q} \in \mathcal{N}(\mathbf{p})} \mathbf{q} \right\|_1}_{\text{Laplacian smoothing}} \underbrace{-\lambda \sum_{t=1}^{T} \|\mathcal{P}_z(\mathbf{G}_t \mathbf{S}_t)\|_2}_{\text{depth control}}$$

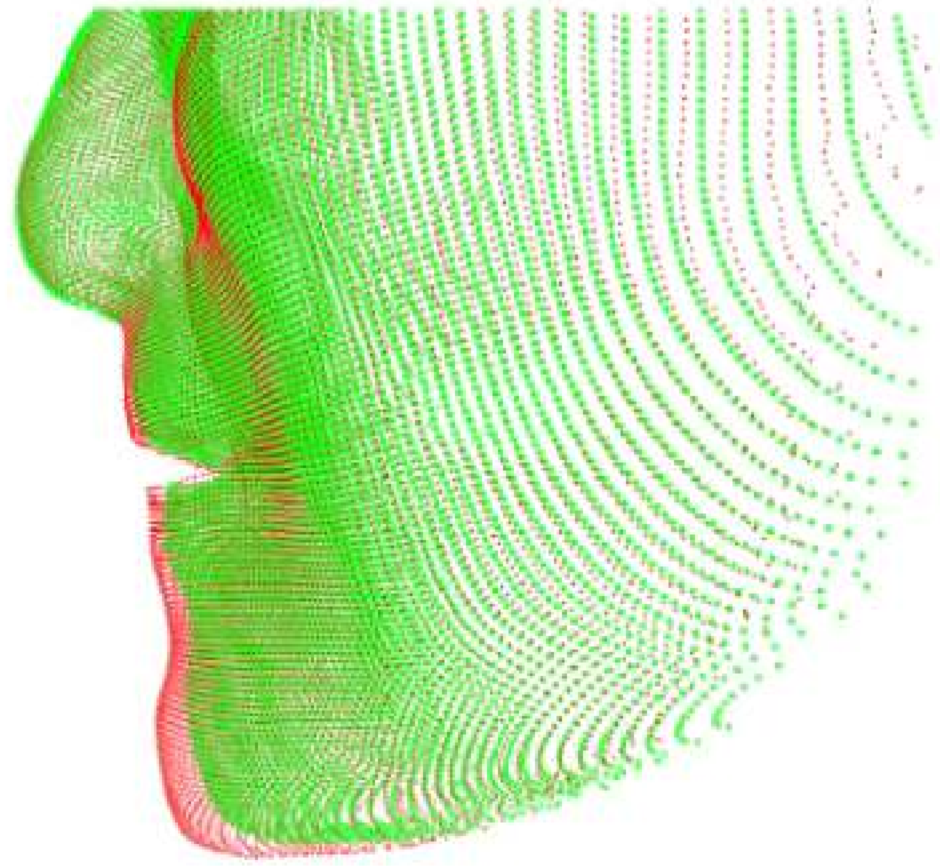

Latent Space Constraints

$$\mathbf{E}_{\text{latent}}(\mathbf{z}) = \|\mathcal{F}(\mathbf{z})\|_1$$

$\mathcal{F}(\cdot)$ denotes the Fourier transform operator

Structure from Recurrent Motion

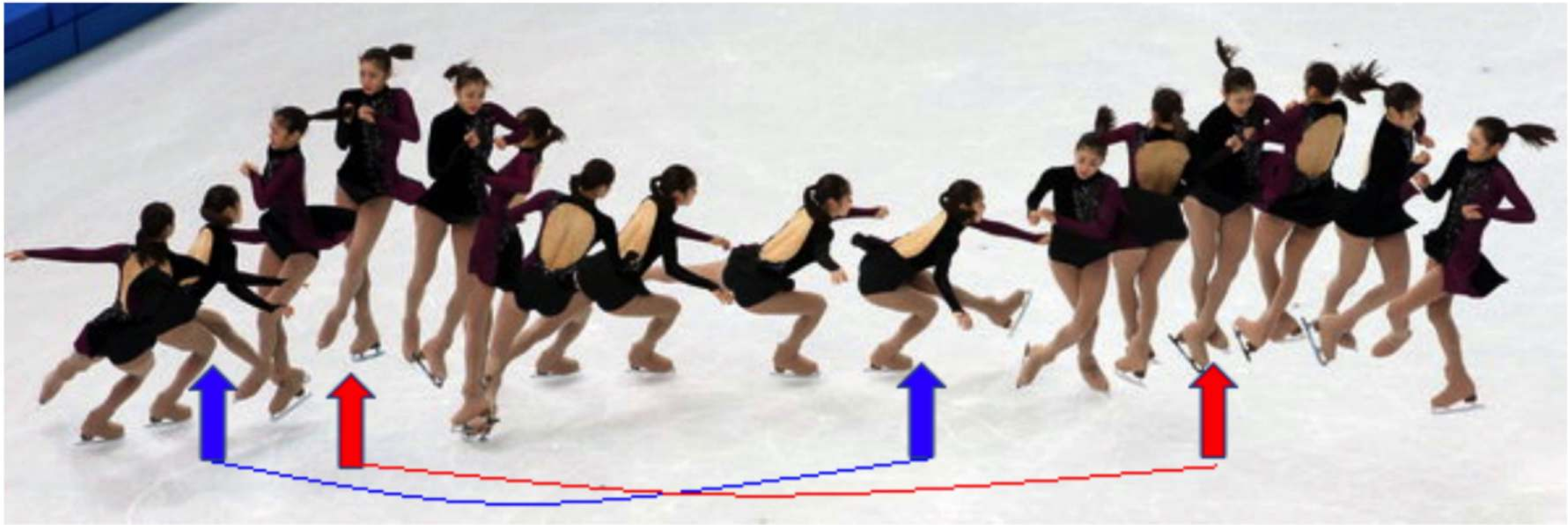

X. Li *et al.*, CVPR, 2018.

Dynamic Shape Prior in NRSfM

V. Golyanik *et al.*, arXiv.org, 2019.

Dynamic Shape Prior in NRSfM

V. Golyanik *et al.*, arXiv.org, 2019.

Dynamic Shape Prior in NRSfM

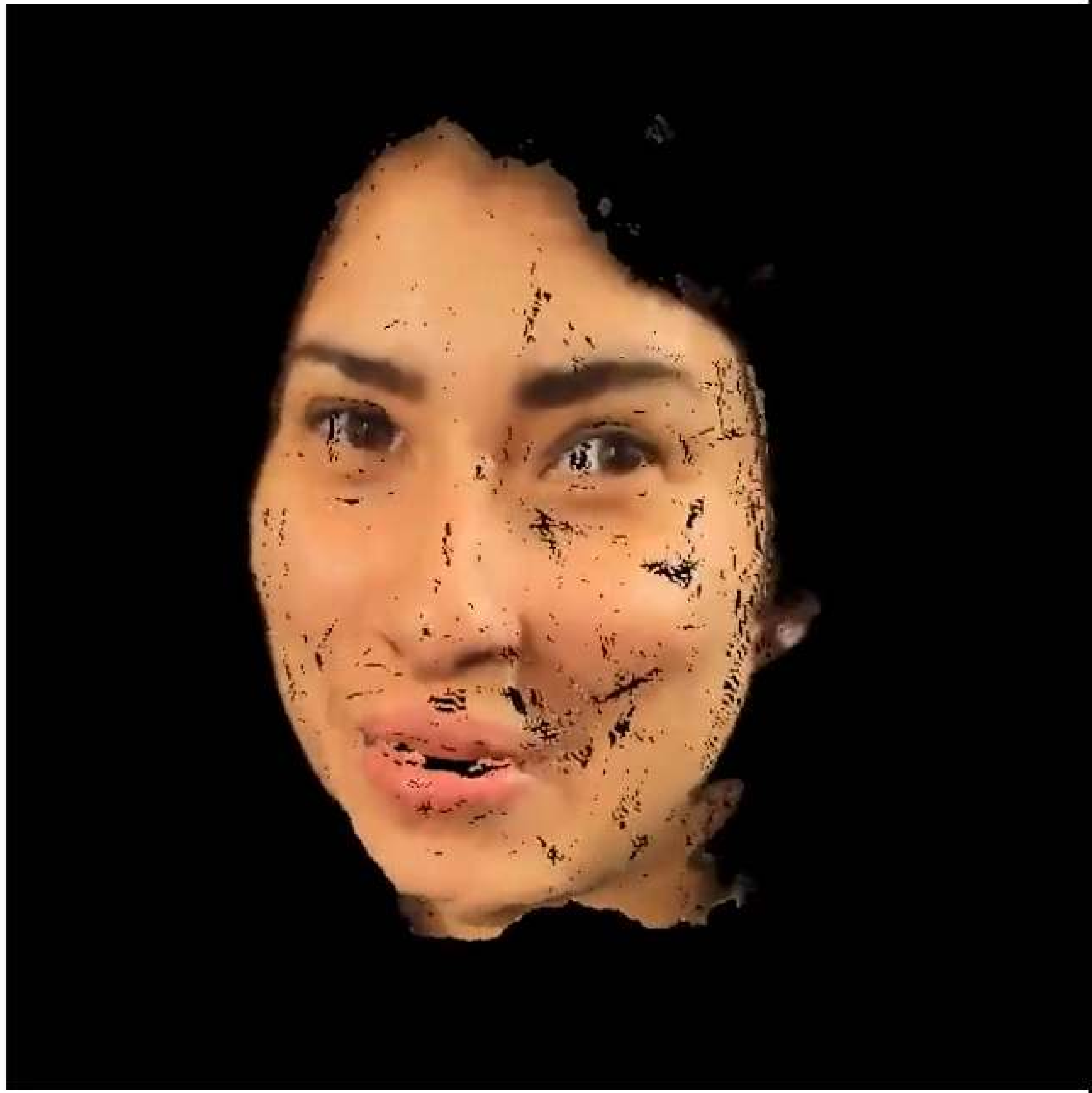

V. Golyanik *et al.*, arXiv.org, 2019.

Latent Space Constraints

$$\mathbf{E}_{\text{latent}}(\mathbf{z}) = \|\mathcal{F}(\mathbf{z})\|_1$$

$\mathcal{F}(\cdot)$ denotes the Fourier transform operator

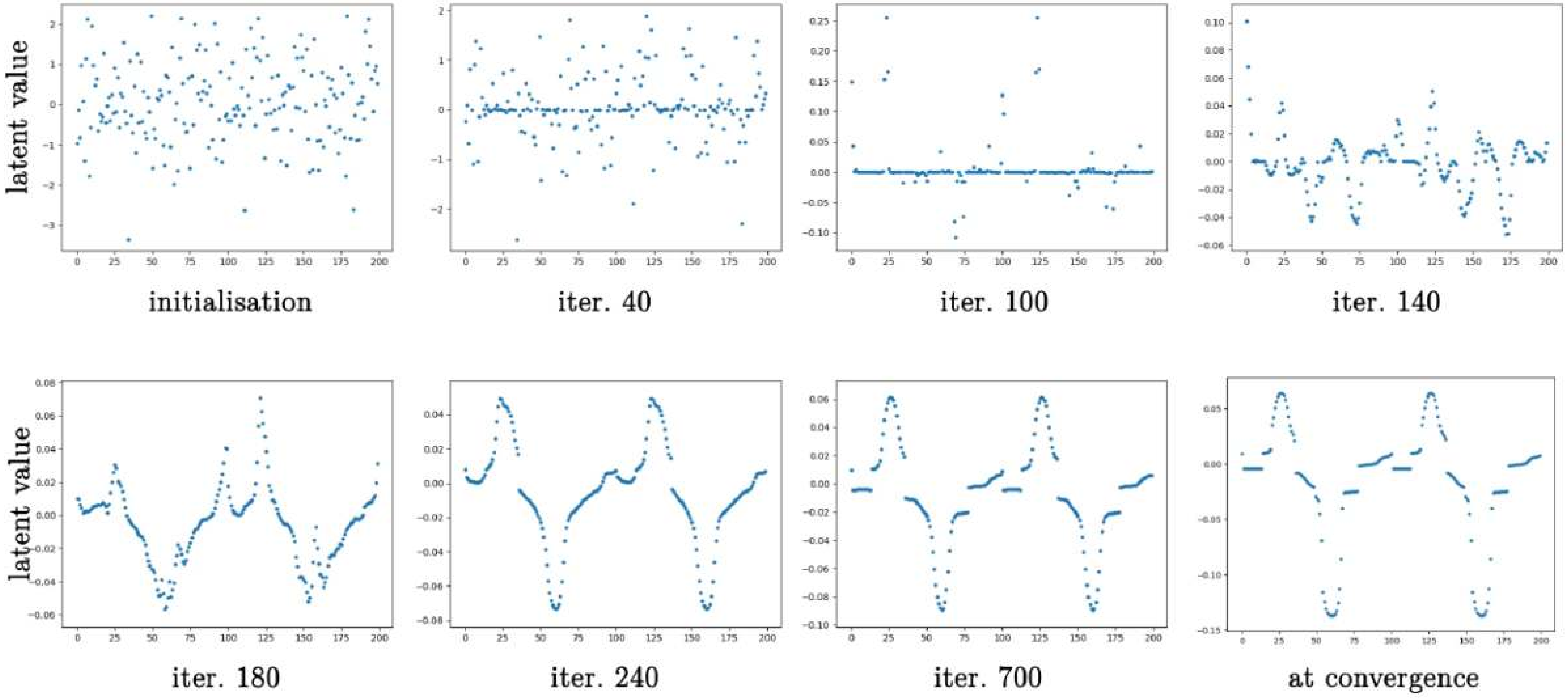

Latent Space Constraints

$$\mathbf{E}_{\text{latent}}(\mathbf{z}) = \|\mathcal{F}(\mathbf{z})\|_1$$

$\mathcal{F}(\cdot)$ denotes the Fourier transform operator

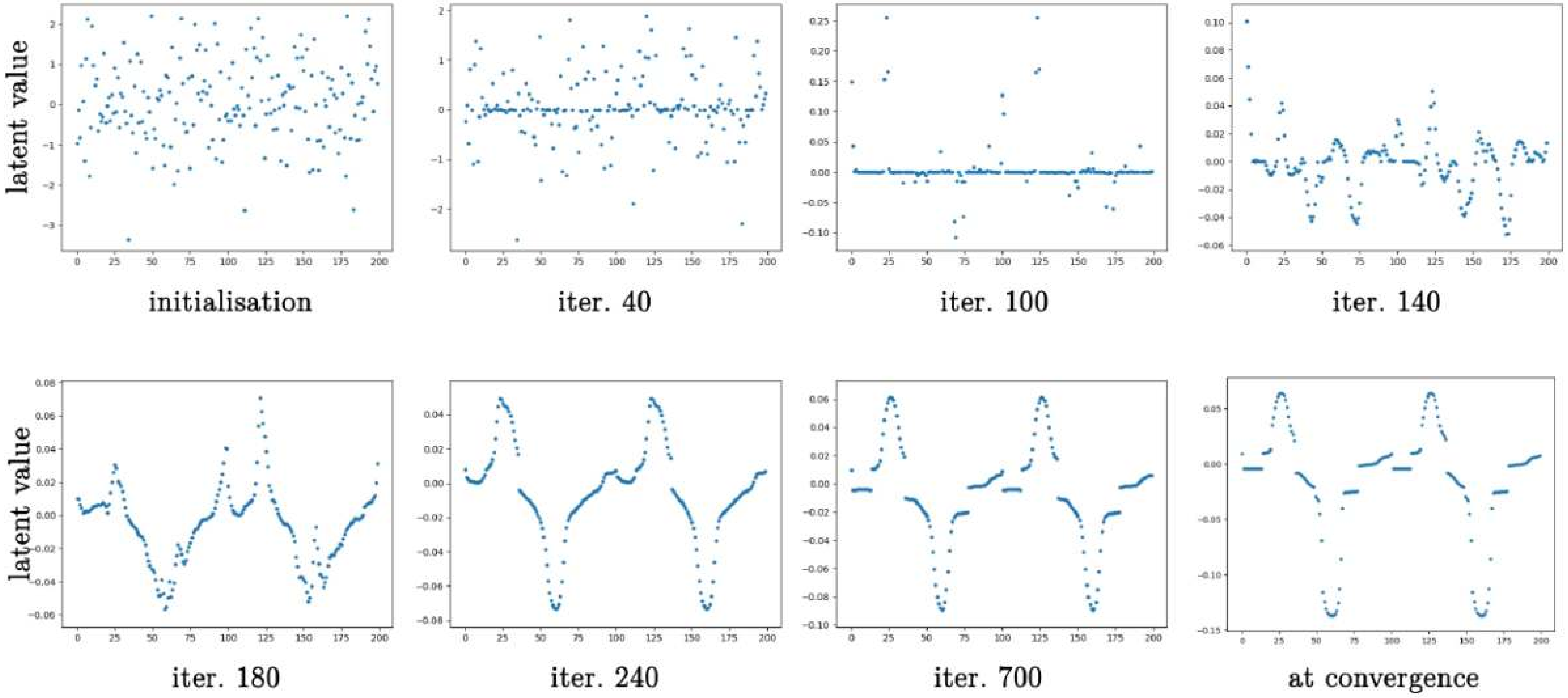

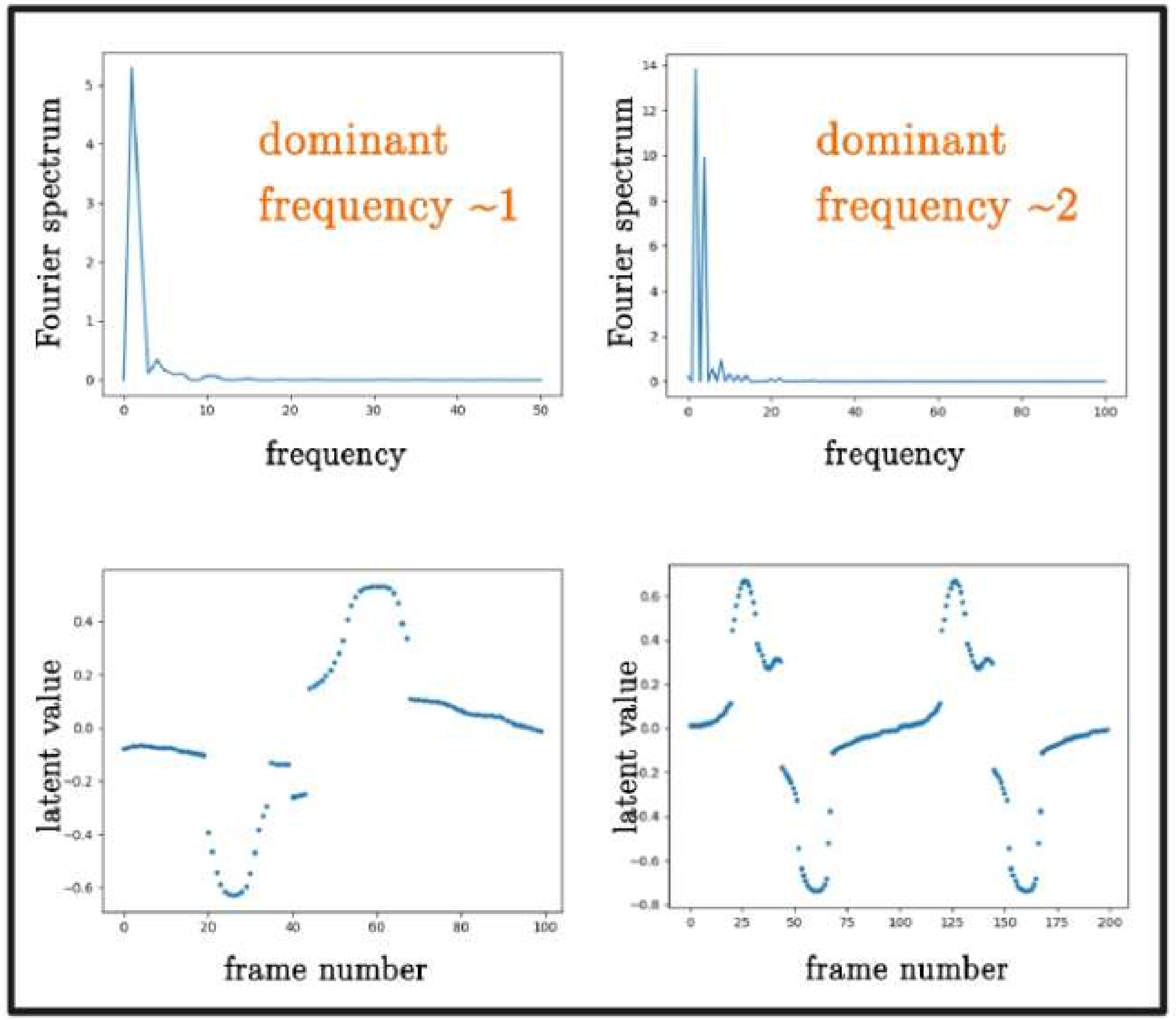

Experimental Results

Synthetic Face Sequences

	TB [7]	MP [43]	VA [19]	DSTA [15]	CDF [23]	CMDR [24]
traj. A	0.1252	0.0611	0.0346	0.0374	0.0886	0.0324
traj. B	0.1348	0.0762	0.0379	0.0428	0.0905	0.0369

	GM* [37]	JM* [36]	SMSR [8]	PPTA [6]	EM-FEM [1]†	N-NRSfM (ours)
traj. A	0.0294	0.0280	0.0304	0.0309	0.0389	0.045 / 0.032$^\flat$
traj. B	0.0309	0.0327	0.0319	0.0572	0.0304	0.049 / 0.0389$^\natural$

[1] A. Agudo *et al.*, Online Dense Non-Rigid 3D Shape and Camera Motion Recovery. BMVC, 2014.
[6] A. Agudo and F. Moreno-Noguer. A Scalable, Efficient, and Accurate Solution to Non-Rigid Structure from Motion. CVIU, 2018.
[7] I. Akhter *et al*. Trajectory space: A dual representation for nonrigid structure from motion. TPAMI, 2011.
[8] M. D. Ansari *et al*. Scalable Dense Monocular Surface Reconstruction. 3DV, 2017.
[15] Y. Dai *et al*. Dense non-rigid structure-from-motion made easy – a spatial-temporal smoothness based solution. ICIP, 2017.
[19] R . Garg *et al*. Dense Variational Reconstruction of Non-Rigid Surfaces from Monocular Video. CVPR, 2013.
[23] V. Golyanik *et al*. Introduction to Coherent Depth Fields for Dense Monocular Surface Recovery. BMVC, 2017.
[24] V. Golyanik *et al*. Consolidating Segmentwise Non-Rigid Structure from Motion. MVA, 2019.
[36] S. Kumar. Jumping Manifolds: Geometry Aware Dense Non-Rigid Structure from Motion. In CVPR, 2019.
[37] S. Kumar *et al*. Scalable Dense Non-rigid Structure-from-Motion: A Grassmannian Perspective. CVPR, 2018.
[43] M. Paladini *et al*. Optimal metric projections for deformable and articulated structure-from-motion. IJCV, 2012.

Synthetic Face Sequences

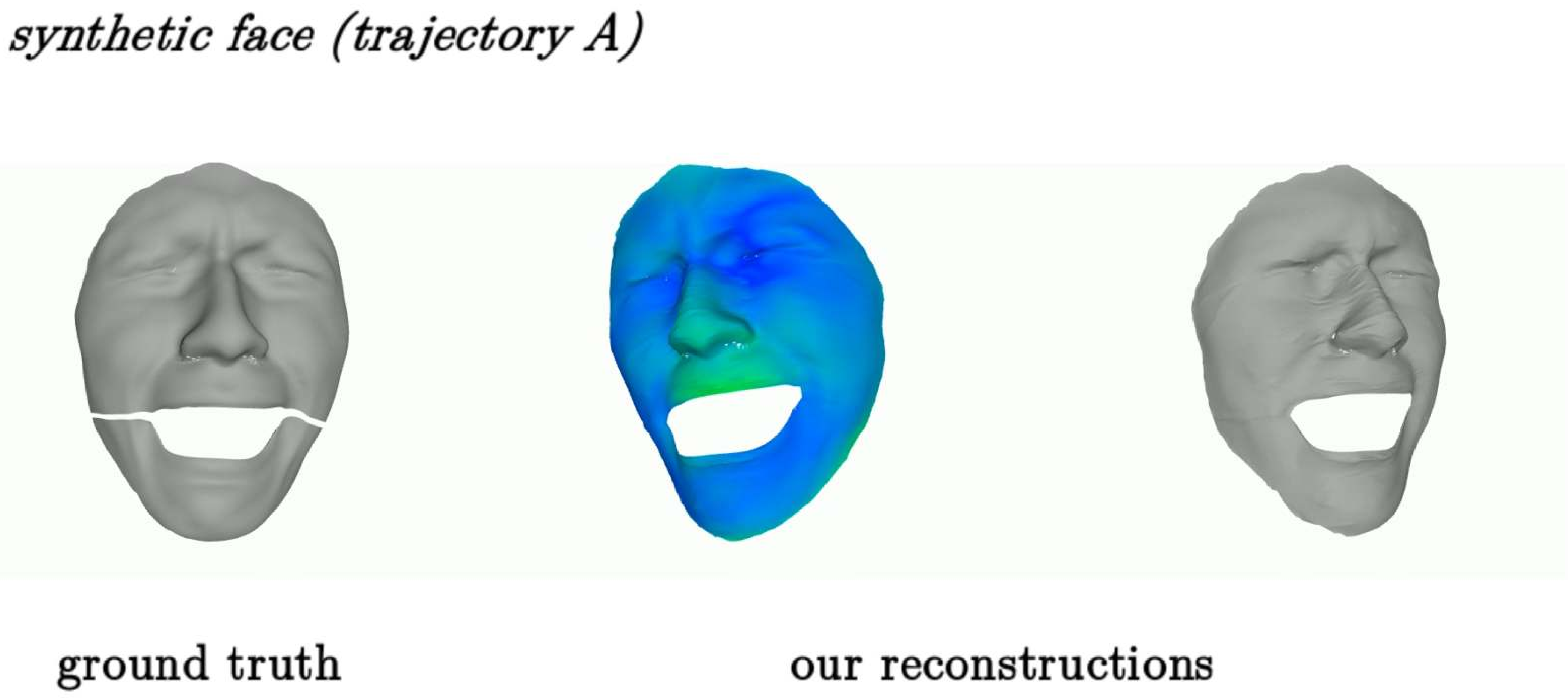

Synthetic Face Sequences

synthetic face (trajectory A)

ground truth our reconstructions

Synthetic Face Sequences

synthetic face (trajectory B)

ground truth   our reconstructions

Expressions Sequence

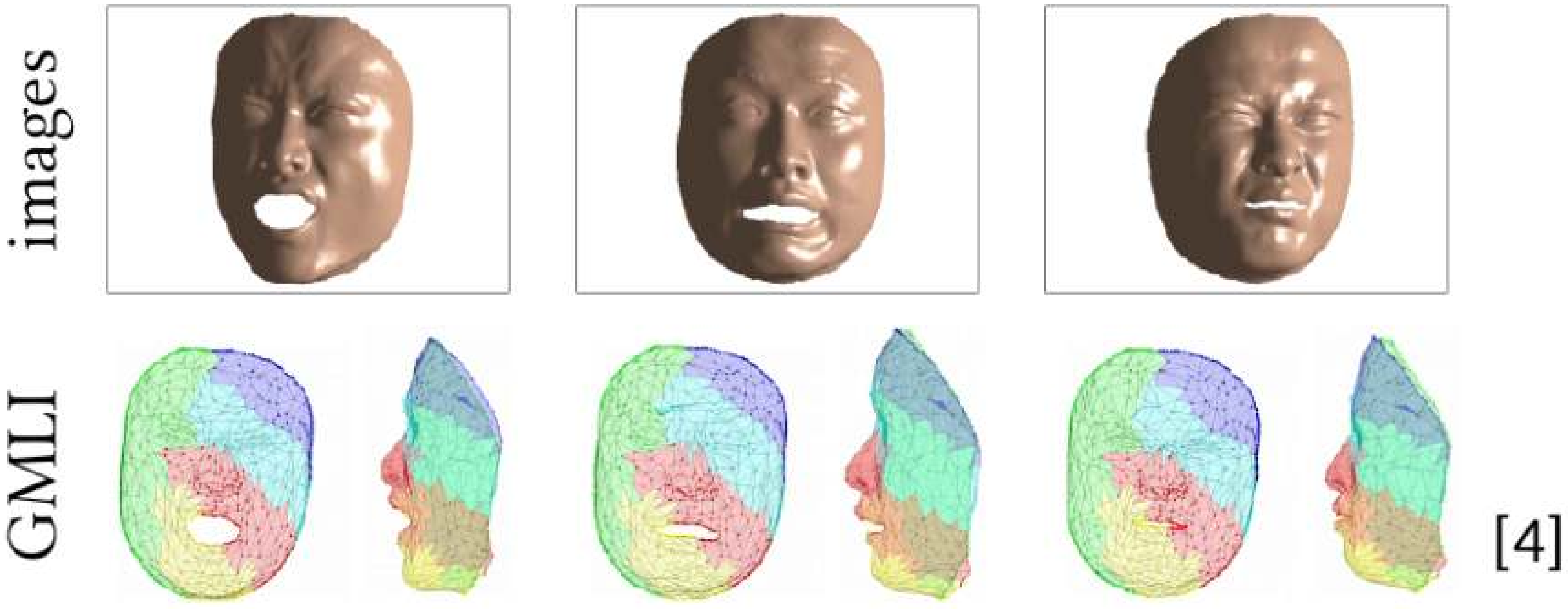

EM-LDS [61]	PTA [7]	CSF2 [29]	KSTA [28]	GMLI [4]	N-NRSfM (ours)
0.044	0.048	0.03	0.035	**0.026**	**0.026**

[4] A. Agudo and F. Moreno-Noguer. Global model with local interpretation for dynamic shape reconstruction. WACV, 2017.
[7] I. Akhter *et al*. Trajectory space: A dual representation for nonrigid structure from motion. TPAMI, 2011.
[28] P. F. U. Gotardo and A. M. Martinez. Kernel non-rigid structure from motion. ICCV, 2011.
[29] P. F. U. Gotardo and A. M. Martinez. Non-rigid structure from motion with complementary rank-3 spaces. CVPR, 2011.
[61] L. Torresani *et al*. Nonrigid structure-from-motion: Estimating shape and motion with hierarchical priors. TPAMI, 2008.

Kinect Paper and T-Shirt

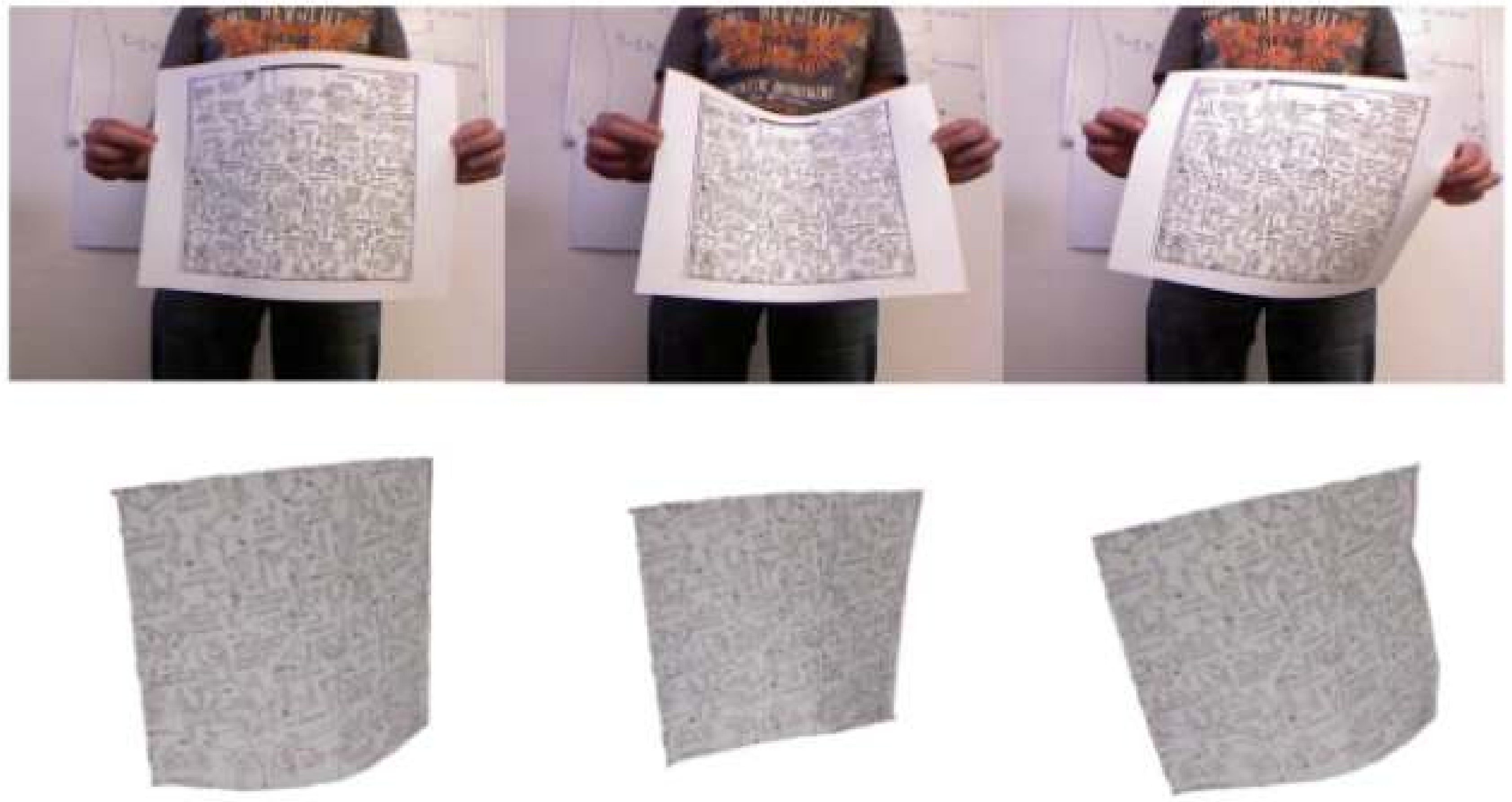

	TB [7]	MP [43]	DSTA [15]	GM [37]	JM [36]	N-NRSfM (ours)
paper	0.0918	0.0827	0.0612	0.0394	0.0338	**0.0332**
t-shirt	0.0712	0.0741	0.0636	0.0362	0.0386	**0.0309**

[7] I. Akhter *et al*. Trajectory space: A dual representation for nonrigid structure from motion. TPAMI, 2011.
[15] Y. Dai *et al*. Dense non-rigid structure-from-motion made easy – a spatial-temporal smoothness based solution. ICIP, 2017.
[36] S. Kumar. Jumping Manifolds: Geometry Aware Dense Non-Rigid Structure from Motion. In CVPR, 2019.
[37] S. Kumar *et al*. Scalable Dense Non-rigid Structure-from-Motion: A Grassmannian Perspective. CVPR, 2018.
[43] M. Paladini *et al*. Optimal metric projections for deformable and articulated structure-from-motion. IJCV, 2012.

Kinect Paper and T-Shirt

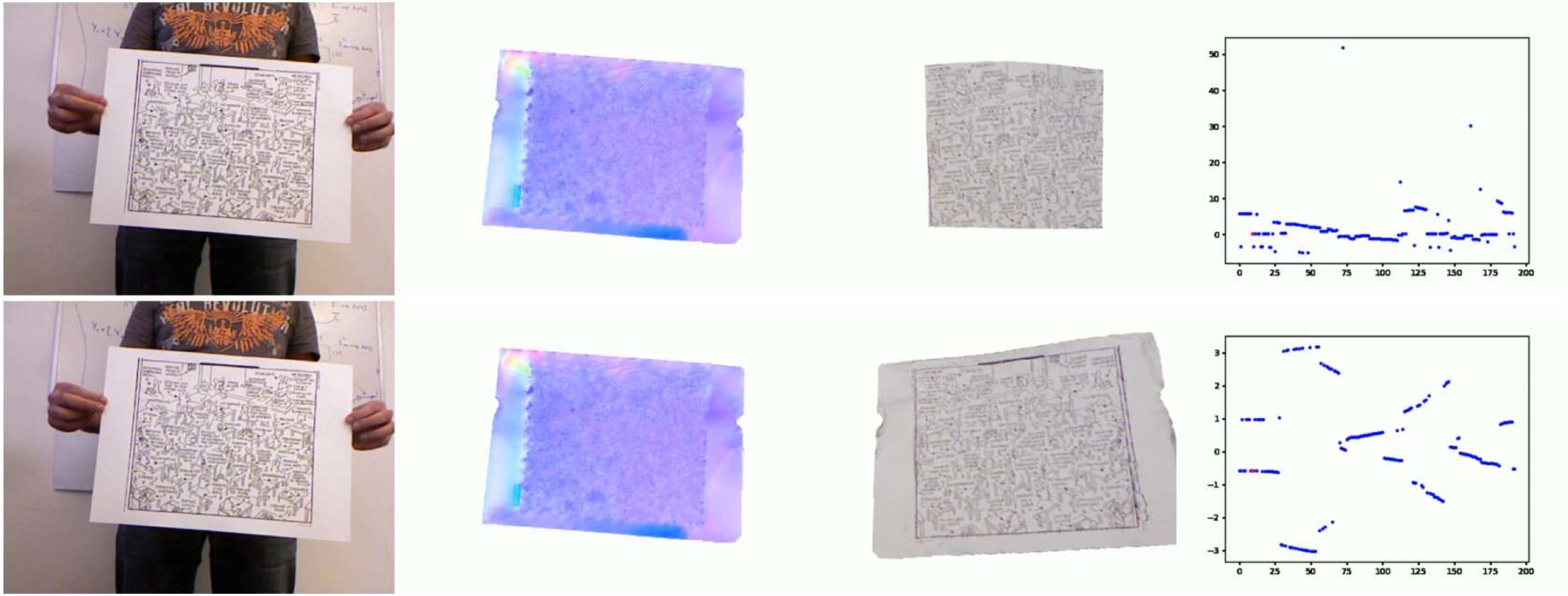

images flow fields 3D reconstructions latent space

Kinect Paper and T-Shirt

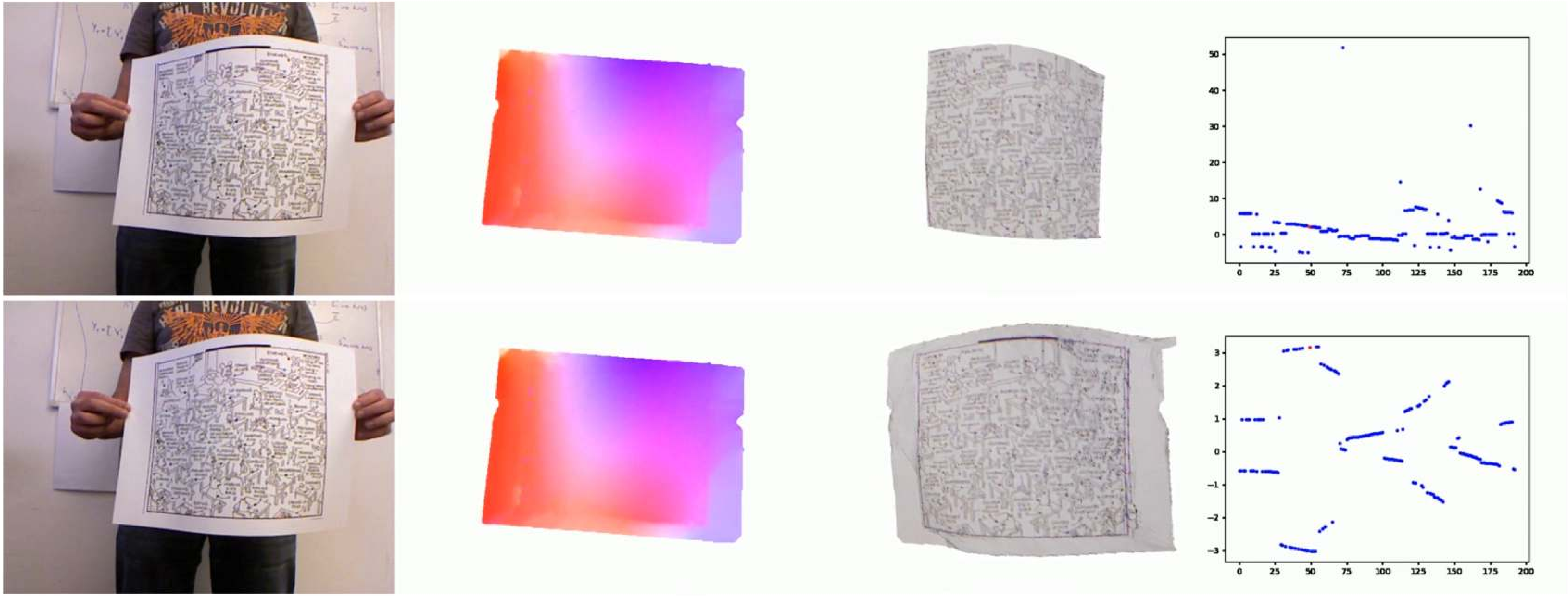

images flow fields 3D reconstructions latent space

Kinect Paper and T-Shirt

images　　flow fields　　3D reconstructions　　latent space

Kinect Paper and T-Shirt

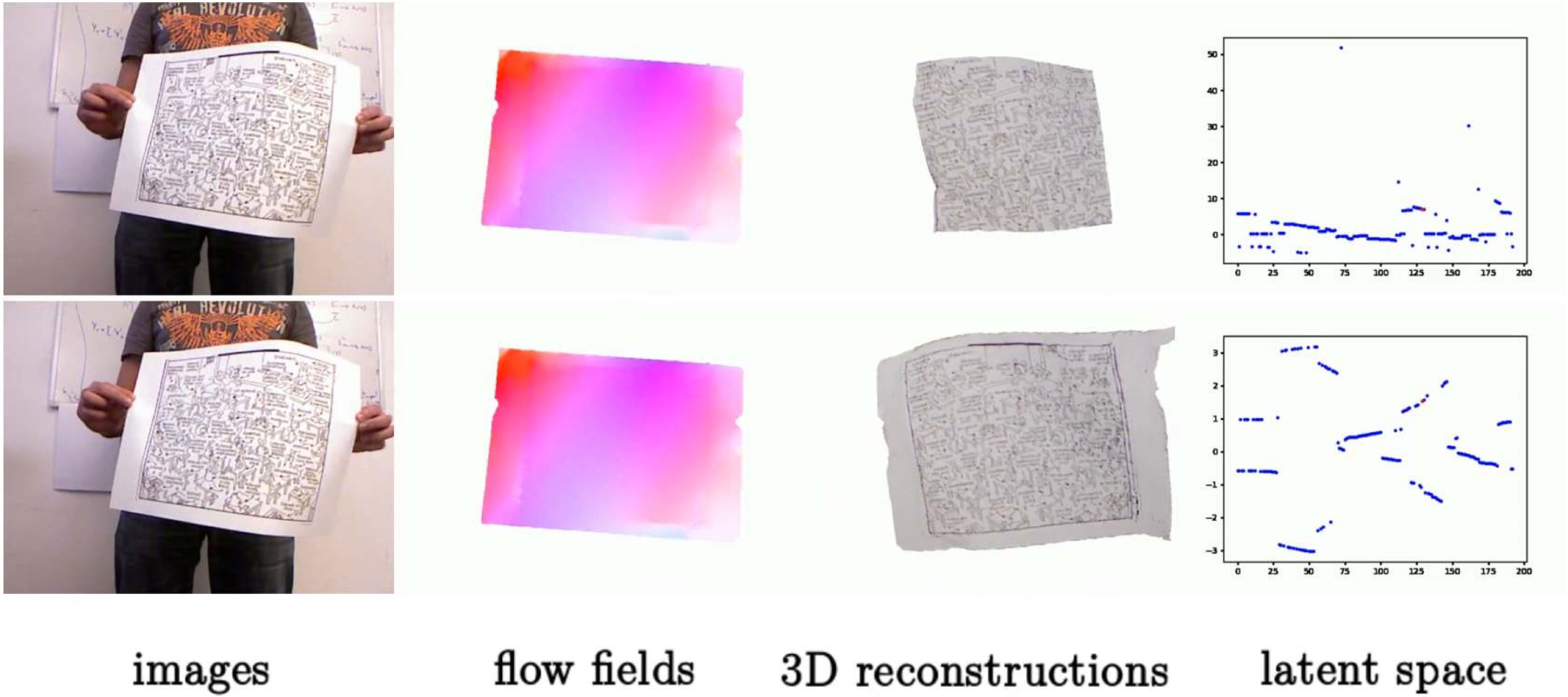

Kinect Paper and T-Shirt

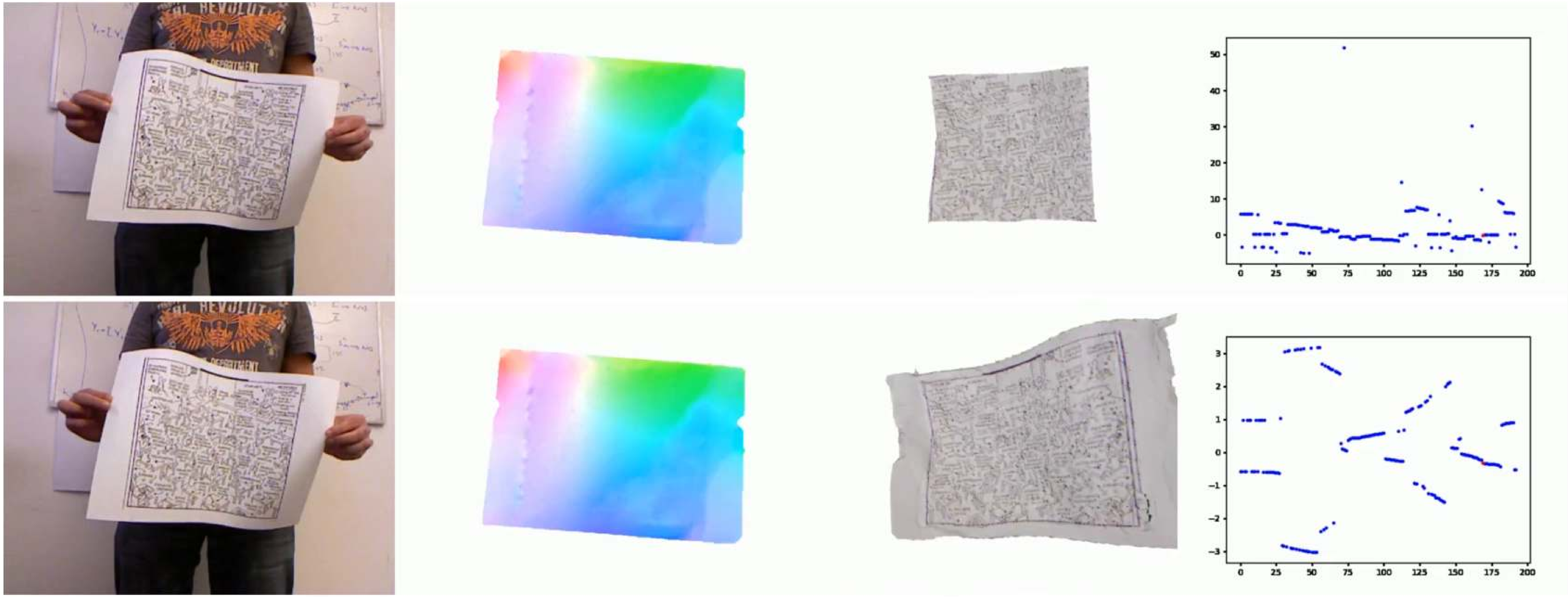

images flow fields 3D reconstructions latent space

Kinect Paper and T-Shirt

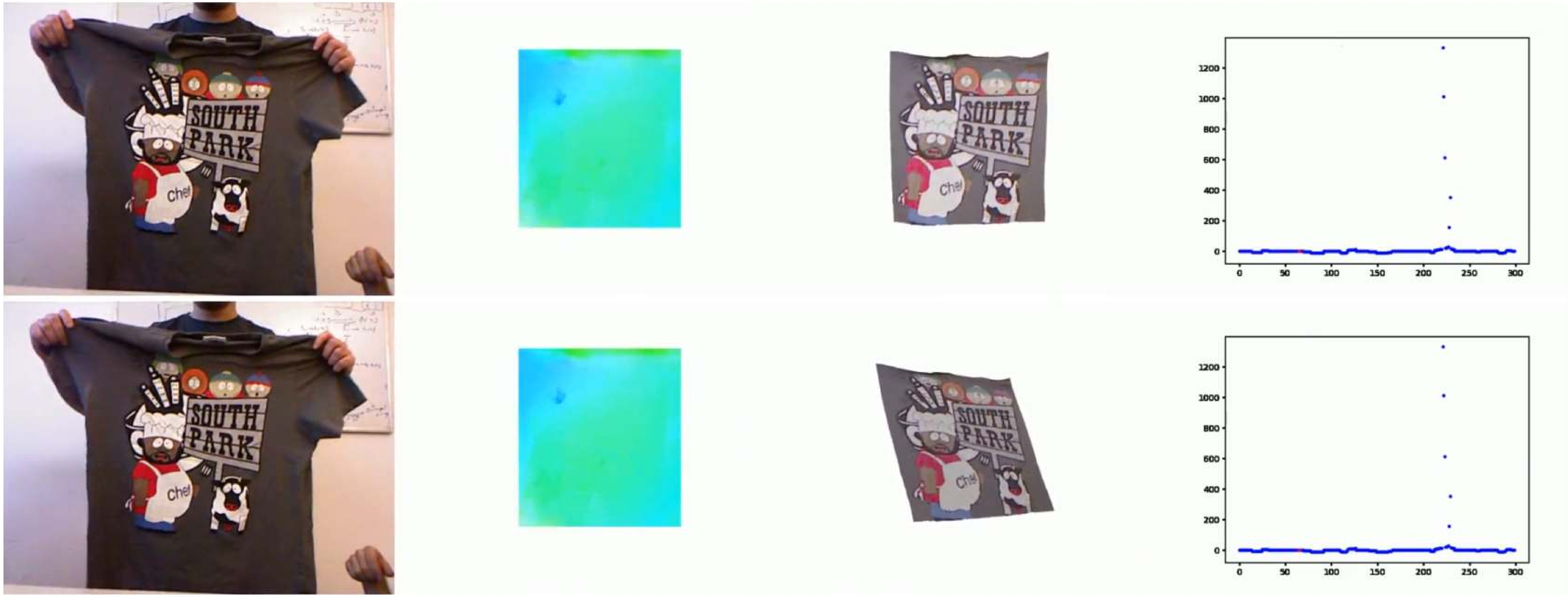

images flow fields 3D reconstructions latent space

Kinect Paper and T-Shirt

images flow fields 3D reconstructions latent space

Comparison to FML

V. Golyanik *et al.*, arXiv.org, 2019.

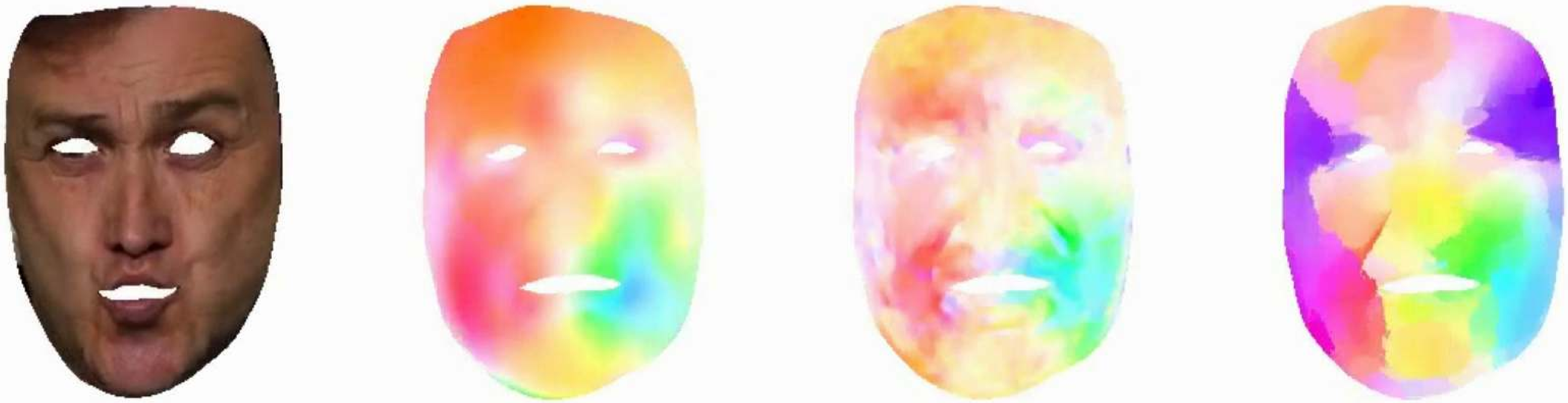

input images GT flow flow computed on images

Comparison to FML

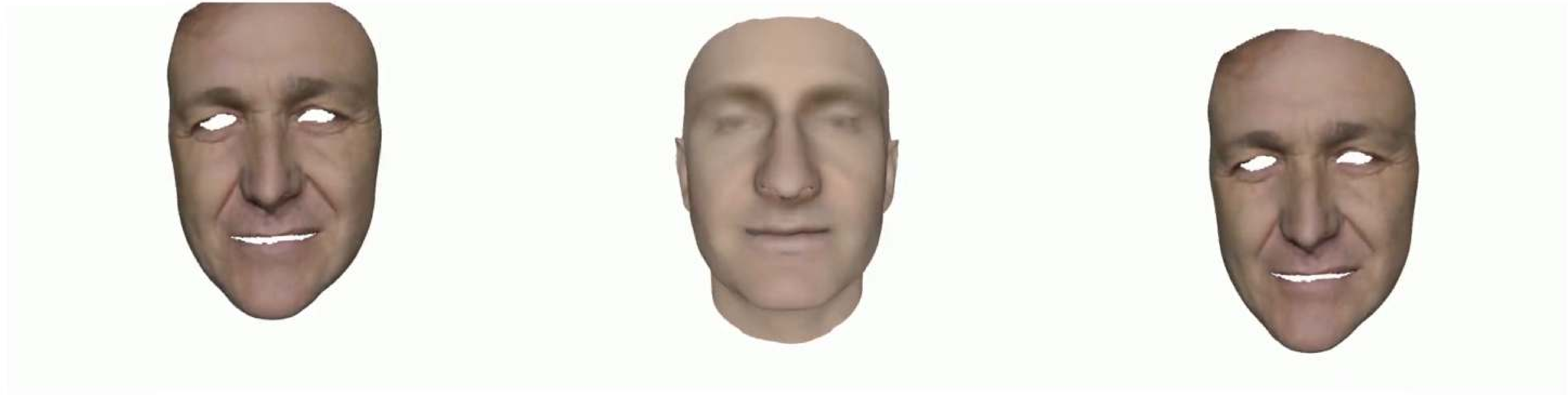

ground truth meshes

FML
Tewari *et al.*, CVPR'19

our reconstructions

A. Tewari *et al*., CVPR, 2019.
V. Golyanik *et al*., arXiv.org, 2019.

Comparison to FML

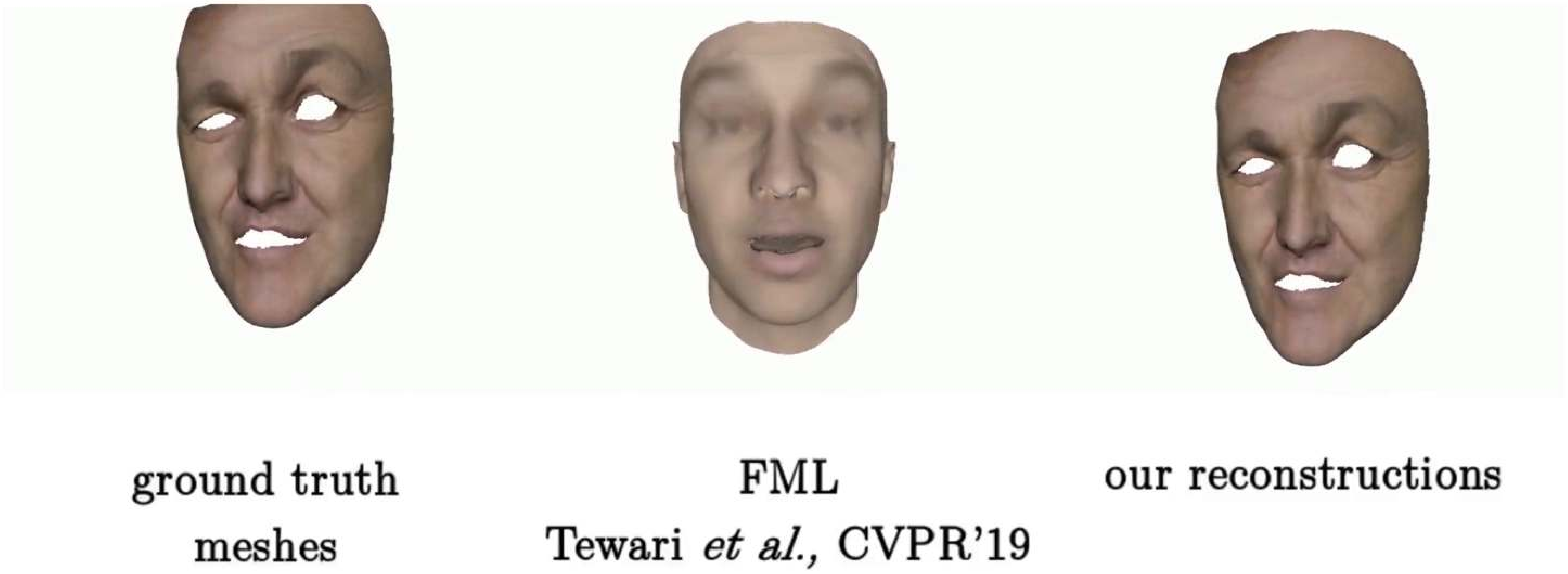

A. Tewari *et al*., CVPR, 2019.
V. Golyanik *et al*., arXiv.org, 2019.

Comparison to FML

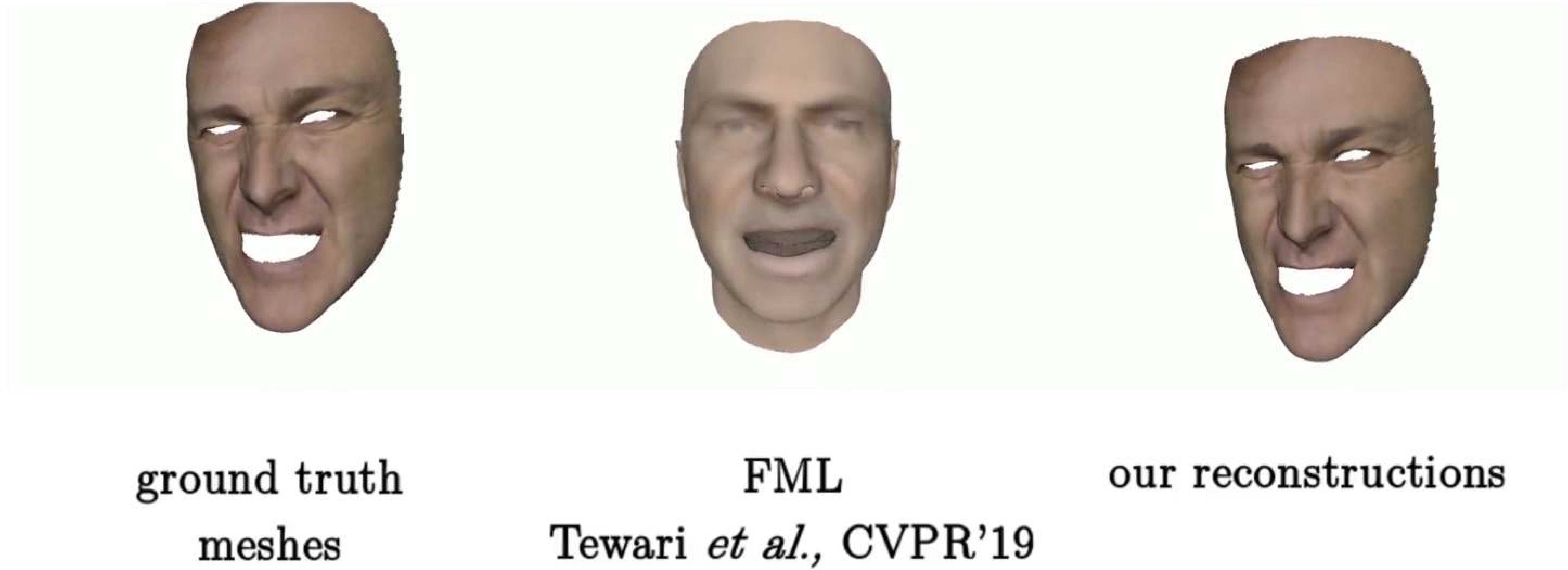

A. Tewari *et al*., CVPR, 2019.
V. Golyanik *et al*., arXiv.org, 2019.

Comparison to FML

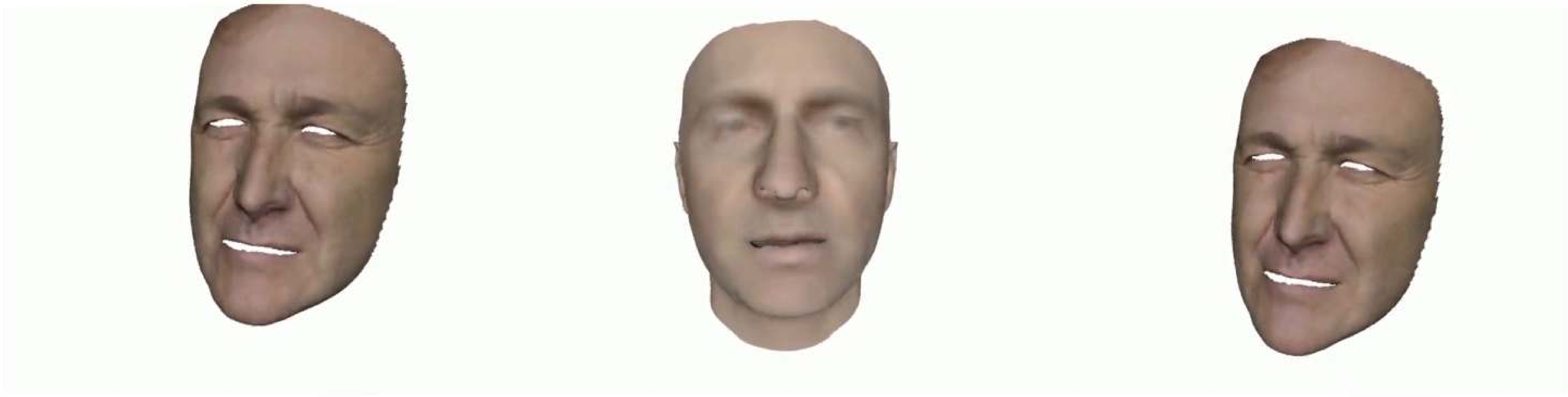

ground truth meshes | FML Tewari *et al.*, CVPR'19 | our reconstructions

A. Tewari *et al.*, CVPR, 2019.
V. Golyanik *et al.*, arXiv.org, 2019.

Experimental Results

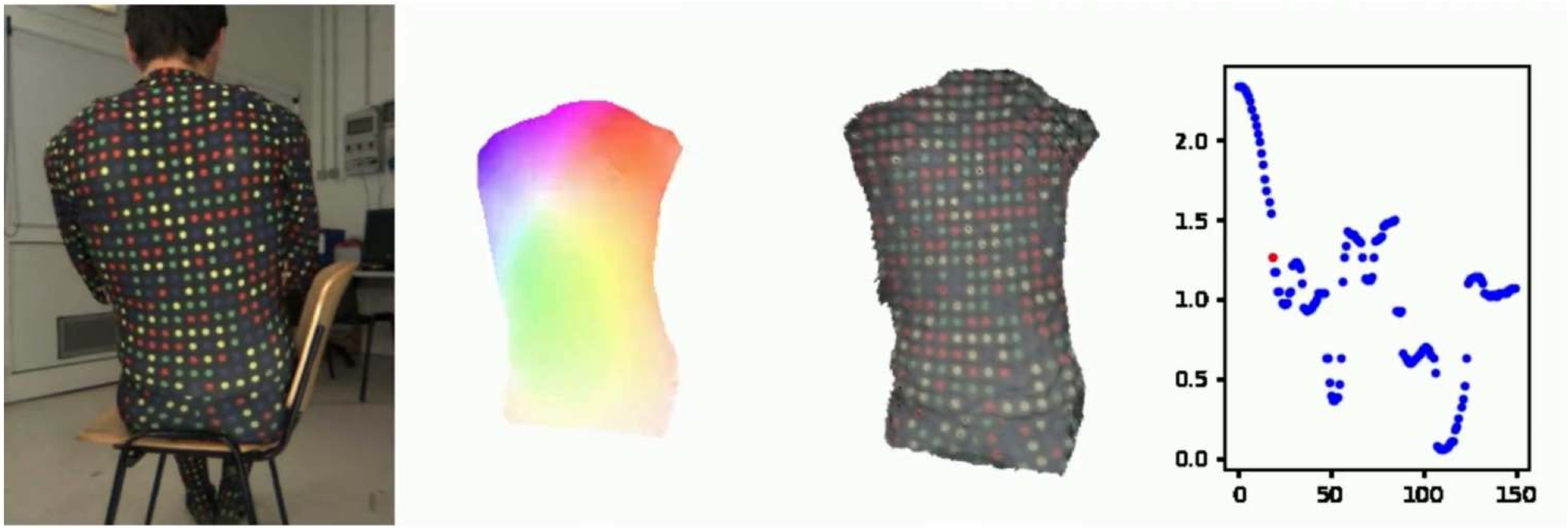

images flow fields 3D reconstructions latent space

Sequence source: C. Russel *et al.*, 3DIMPVT, 2012.

Experimental Results

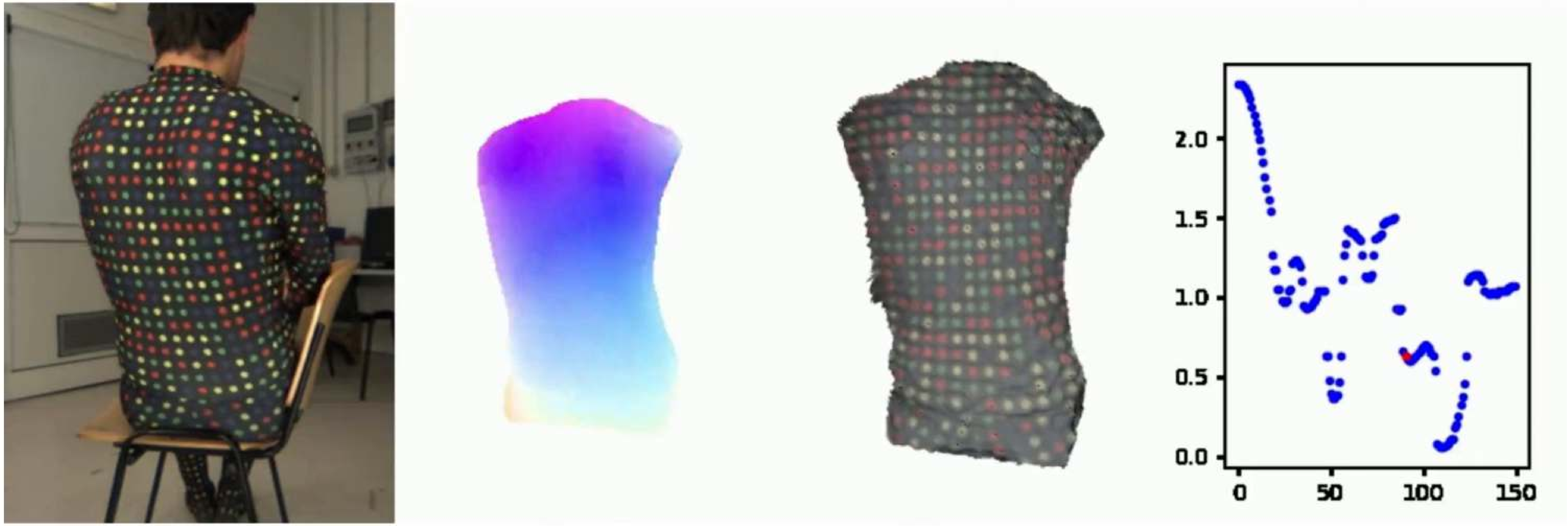

images flow fields 3D reconstructions latent space

Sequence source: C. Russel *et al.*, 3DIMPVT, 2012.

Experimental Results

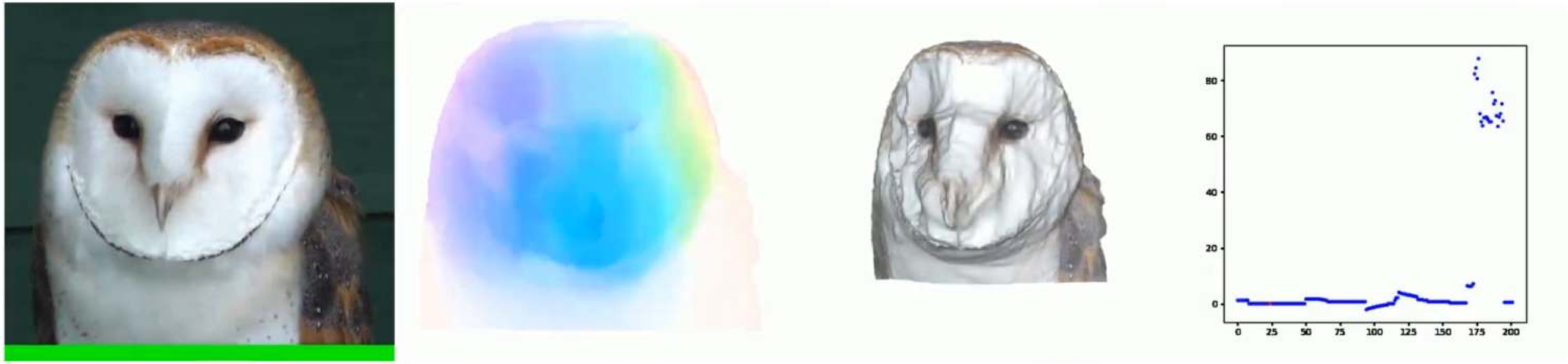

images　　flow fields　　3D reconstructions　　latent space

Sequence source: V. Golyanik *et al*., BMVC, 2016.

Experimental Results

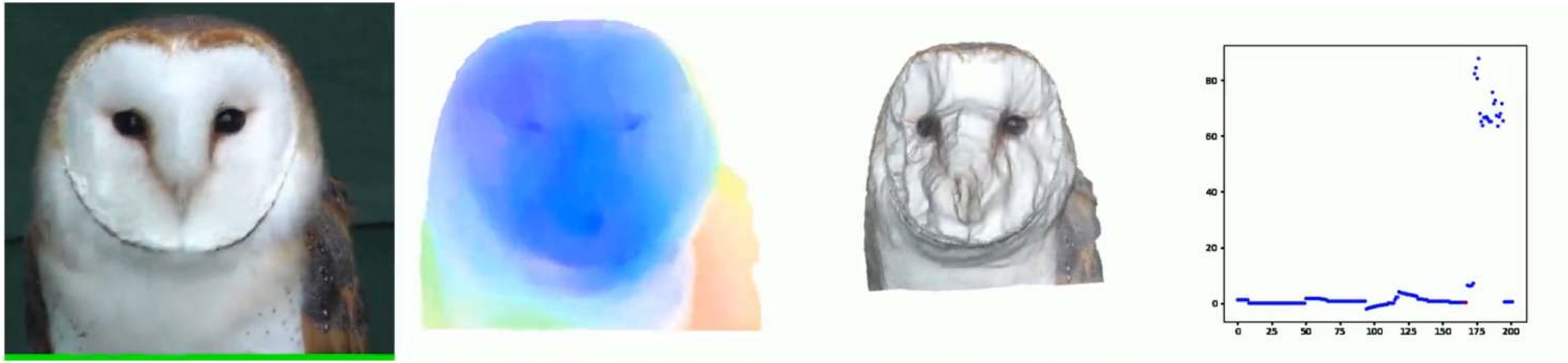

images flow fields 3D reconstructions latent space

Sequence source: V. Golyanik *et al.*, BMVC, 2016.

Experimental Results

input images | no $\mathbf{E}_{\text{spat}}$ | with $\mathbf{E}_{\text{spat}}$

Sequence source: R. Garg *et al*., CVPR, 2013.

Experimental Results

input images — no $\mathbf{E}_{\text{spat}}$ — with $\mathbf{E}_{\text{spat}}$

Sequence source: R. Garg *et al*., CVPR, 2013.

Experimental Results

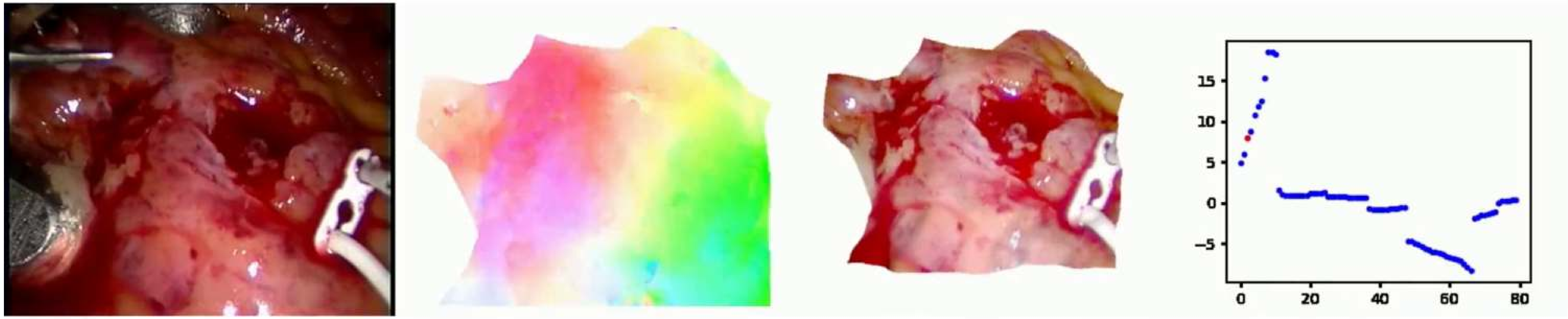

images flow fields 3D reconstructions latent space

Sequence source: D. Stoyanov, MICCAI, 2012.

Experimental Results

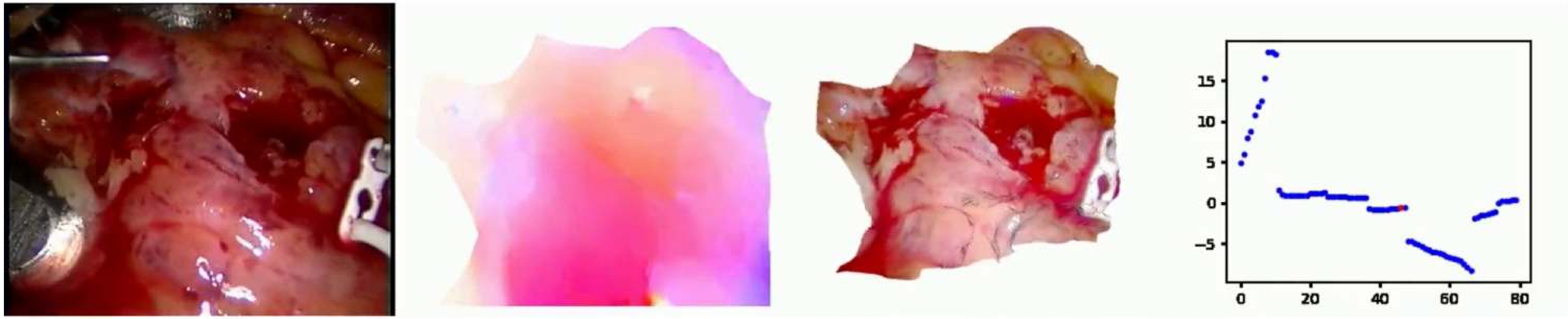

images flow fields 3D reconstructions latent space

Sequence source: D. Stoyanov, MICCAI, 2012.

Experimental Results

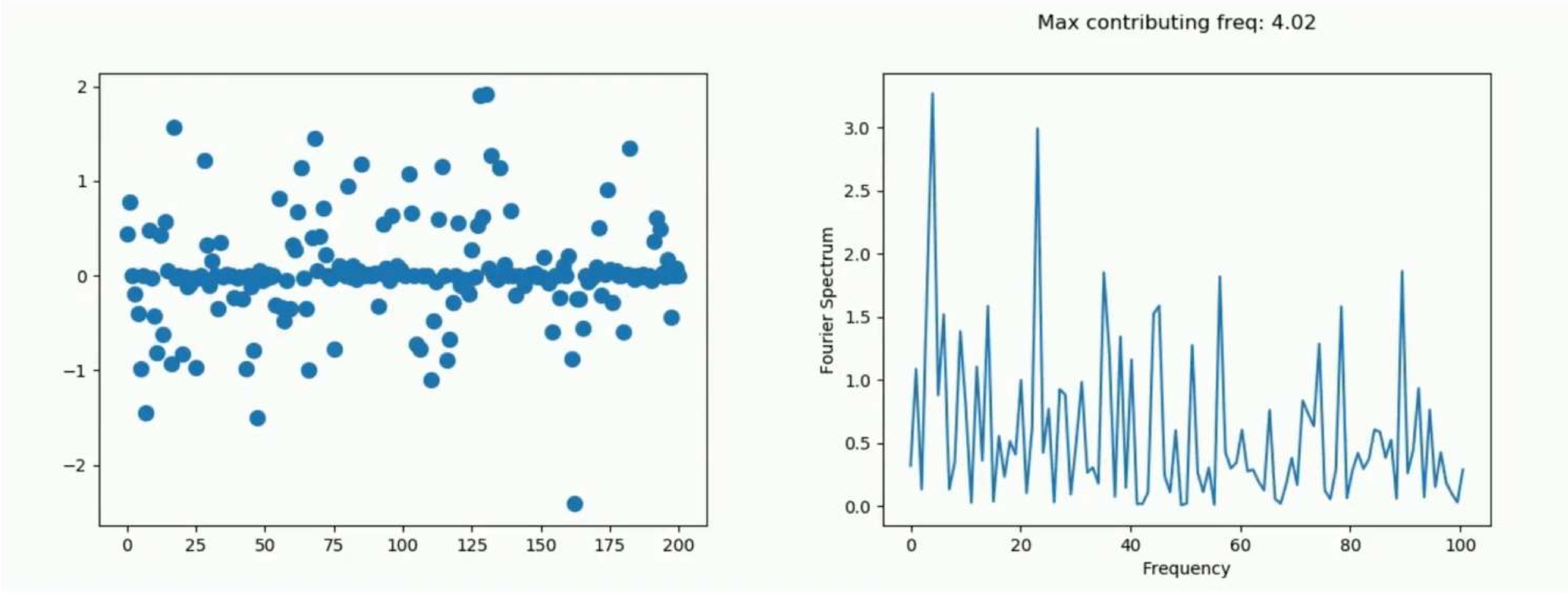

Sequence source: D. Stoyanov, MICCAI, 2012.

Experimental Results

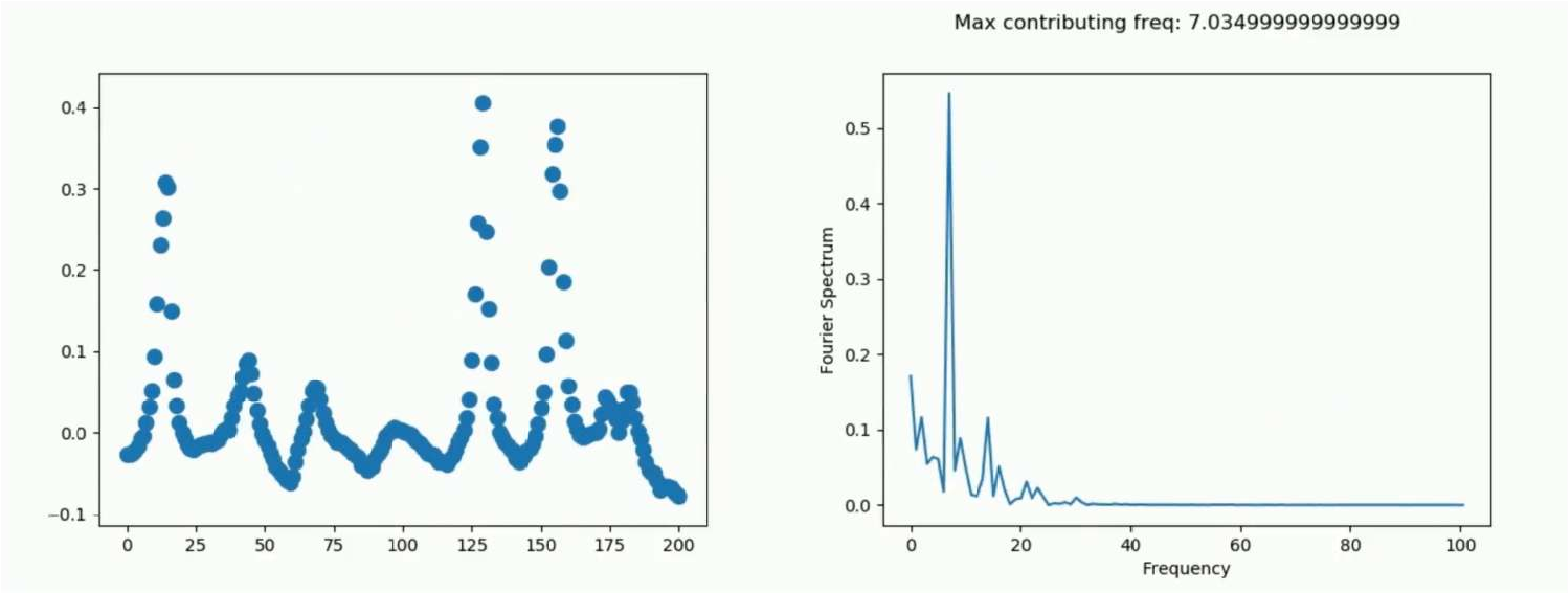

Sequence source: D. Stoyanov, MICCAI, 2012.

Experimental Results

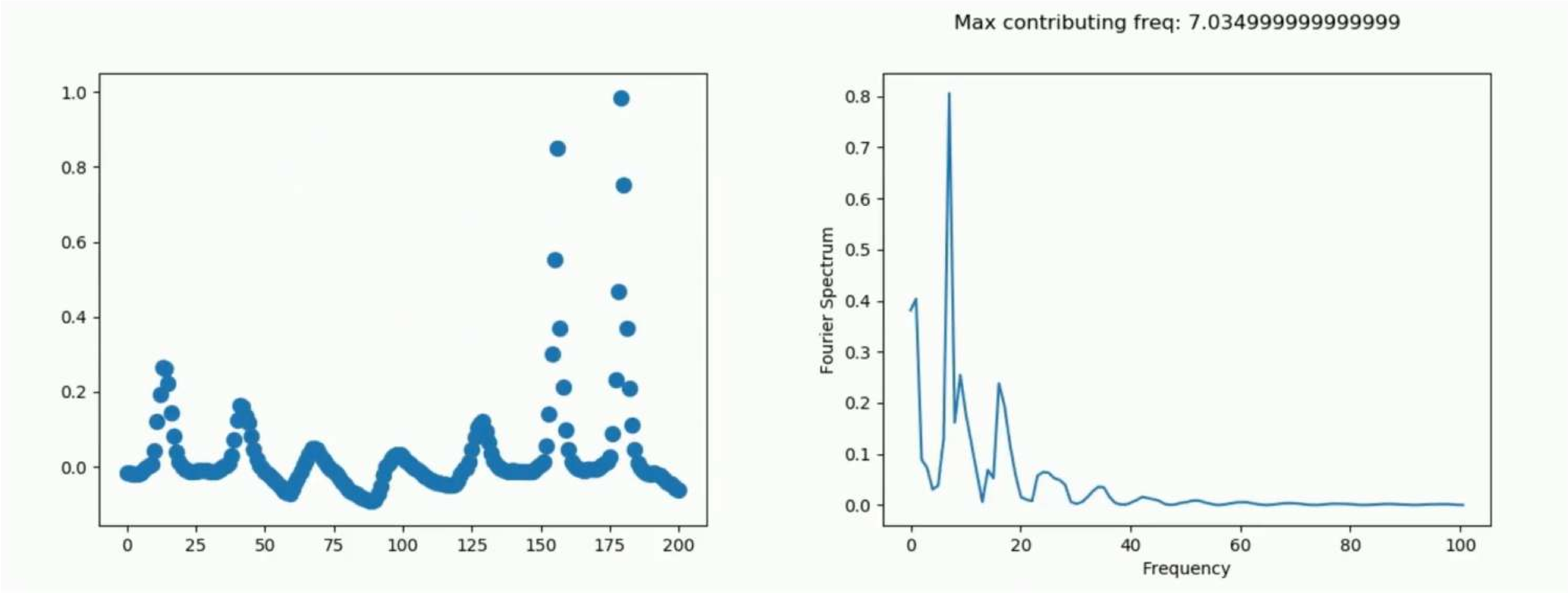

Sequence source: D. Stoyanov, MICCAI, 2012.

Experimental Results

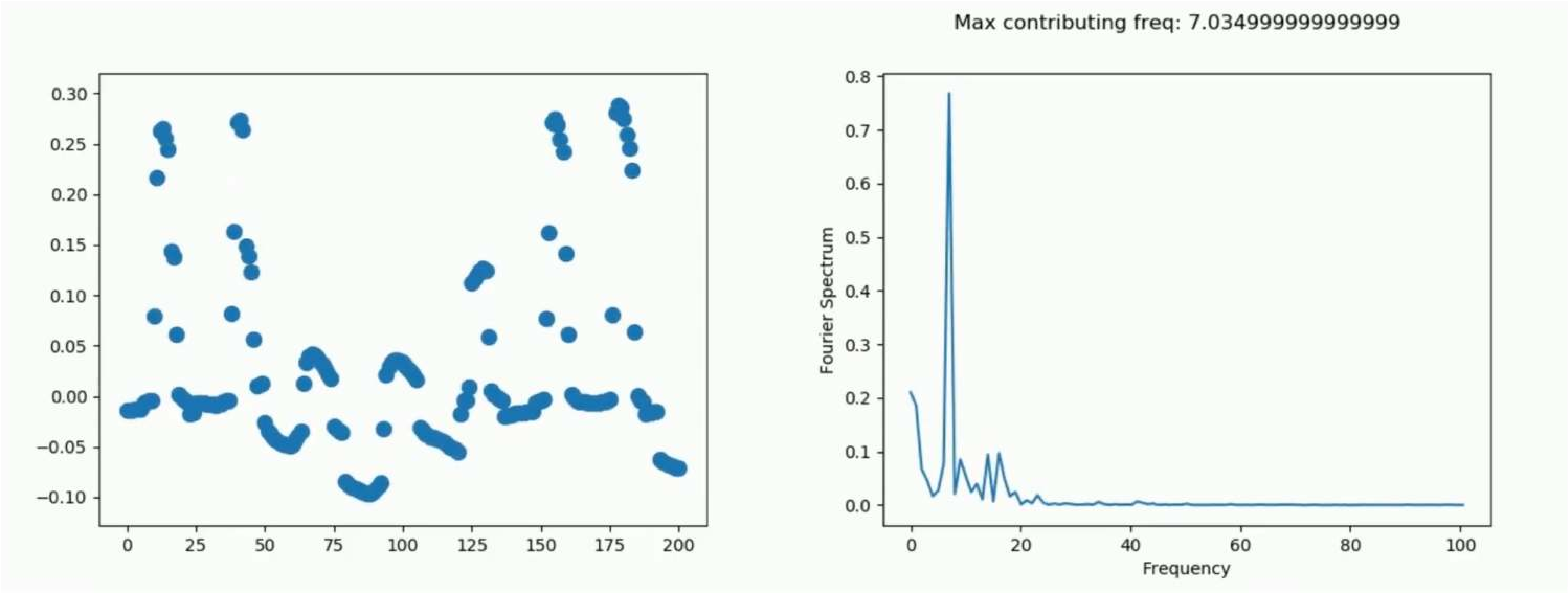

** shown with the increased frame rate*

Sequence source: D. Stoyanov, MICCAI, 2012.

Applications

ground truth

input
(noisy point cloud)

completed shape

Applications

ground truth

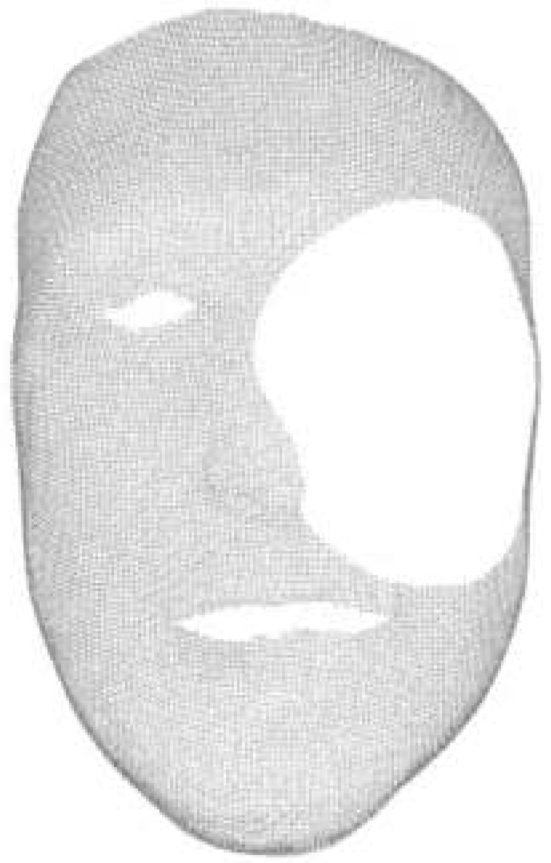

input
(partial point cloud)

completed shape

Applications

ground truth

input
(partial point cloud)

completed shape

Applications

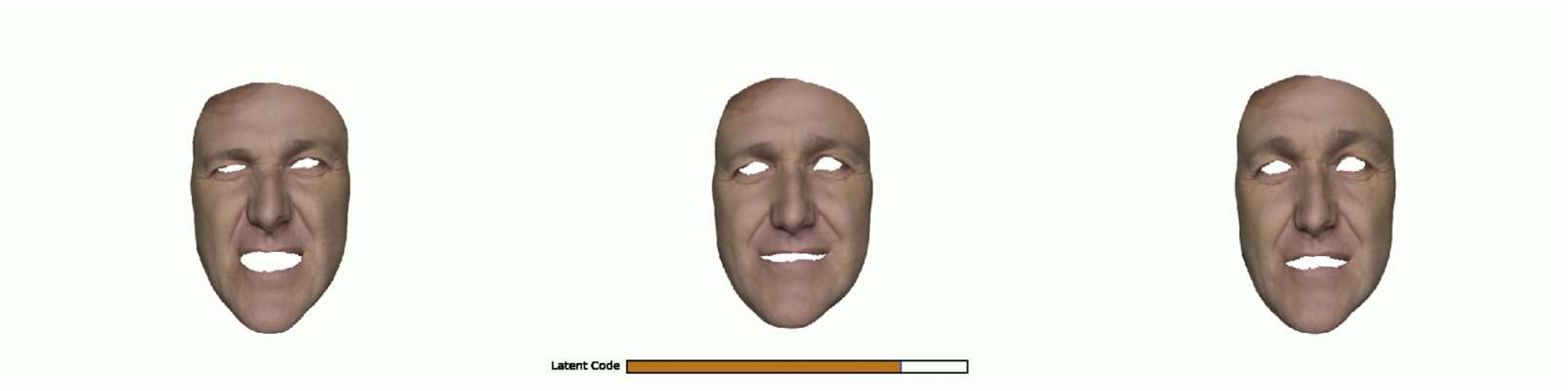

Applications

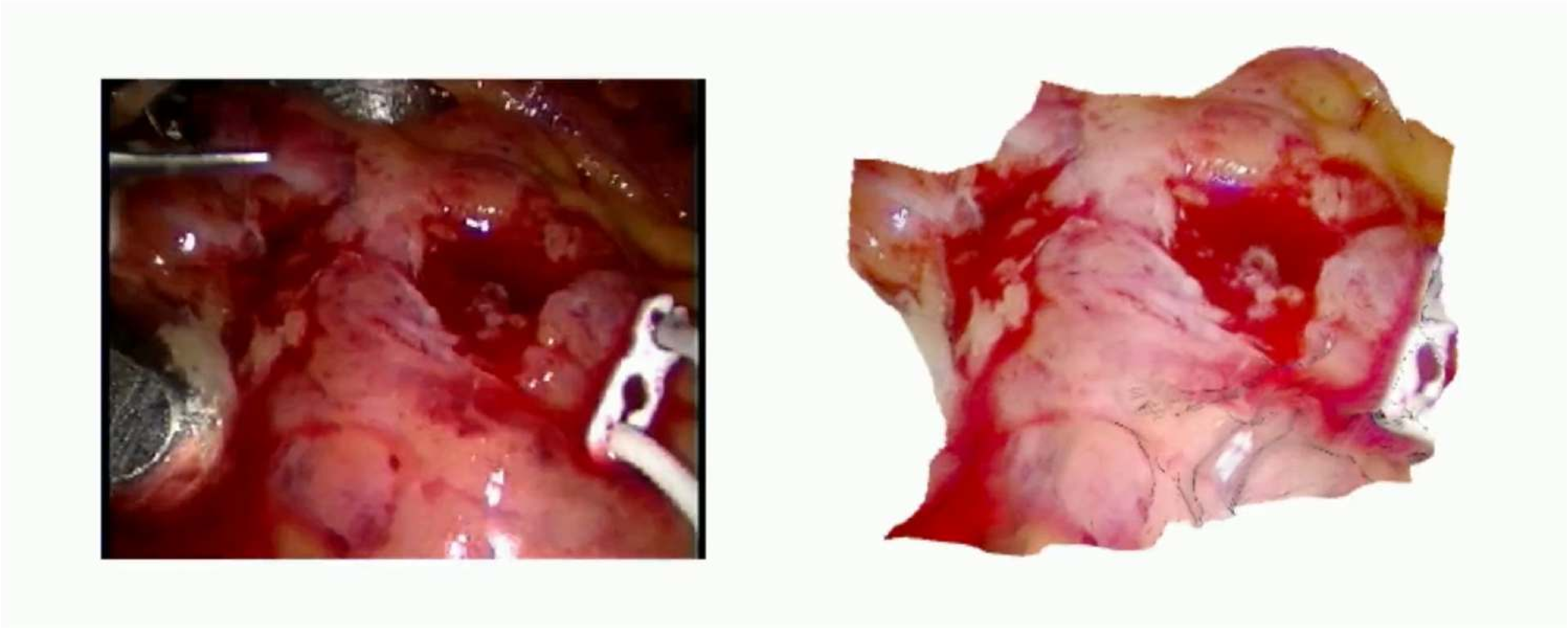

direct monocular non-rigid 3D reconstruction

Applications

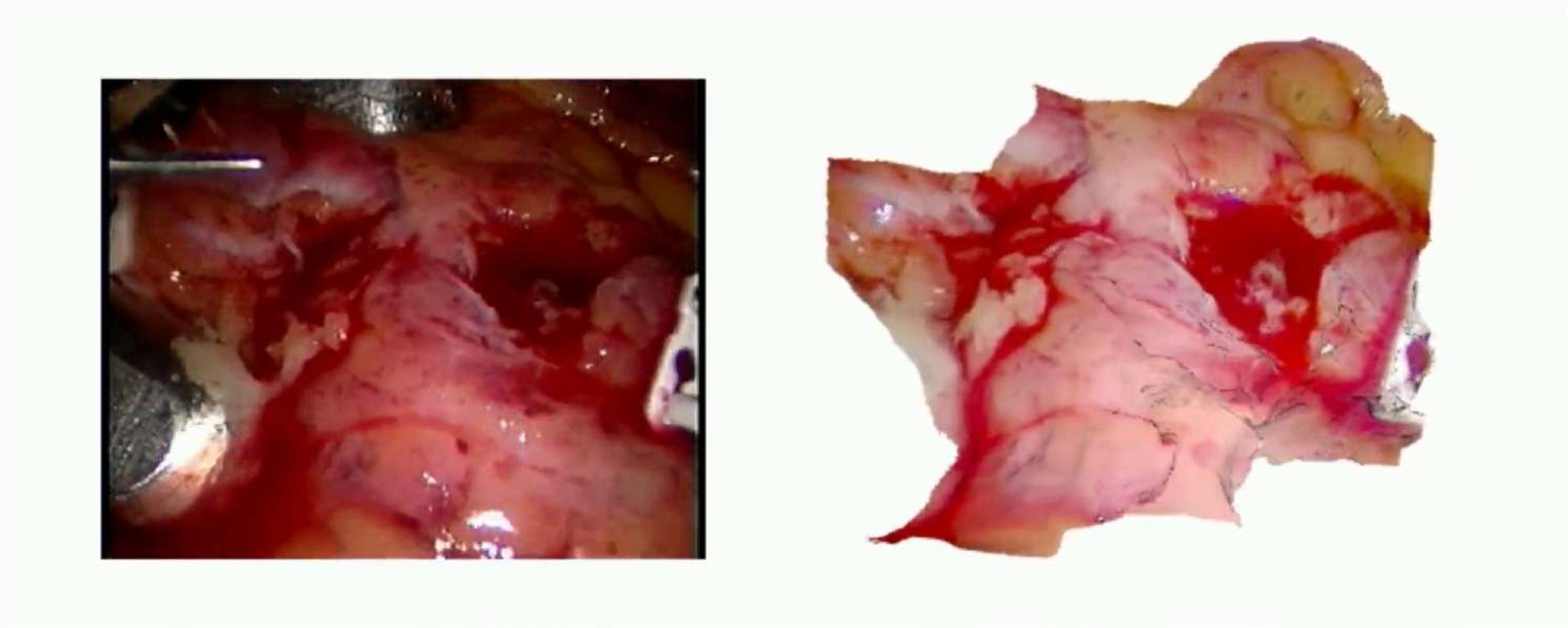

direct monocular non-rigid 3D reconstruction

Project Page

http://gvv.mpi-inf.mpg.de/projects/Neural_NRSfM/

Project Page

http://gvv.mpi-inf.mpg.de/projects/Neural_NRSfM/

source code available for research purposes

ECCV'20 ONLINE
23-28 AUGUST 2020

Thank You

Vikram

Edgar

Antonio

Christian

max planck institut informatik

aarland Informatics Campus SIC

UNIVERSITÄT DES SAARLANDES

Institut de Robòtica i Informàtica Industrial

erc European Research Council

ECCV'20 ONLINE
23-28 AUGUST 2020

Neural Dense Non-Rigid Structure from Motion with Latent Space Constraints

Vikramjit Sidhu [1, 2] Edgar Tretschk [1]
Vladislav Golyanik [1] Antonio Agudo [3] Christian Theobalt [1]

[1] Max Planck Institute for Informatics, SIC [2] Saarland University, SIC
[3] Institut de Robòtica i Informàtica Industrial, CSIC-UPC